

Mono{hydrotris(mercaptoimidazolyl)borato} Complexes of Manganese(II), Iron(II), Cobalt(II), and Nickel(II) Halides

Shunsuke Senda, Yasuhiro Ohki, Tomoko Hirayama, Daisuke Toda, Jing-Lin Chen, Tsuyoshi Matsumoto, Hiroyuki Kawaguchi,[†] and Kazuyuki Tatsumi*

Department of Chemistry, Graduate School of Science and Research Center for Materials Science, Nagoya University, Furo-cho, Chikusa-ku, Nagoya 464-8602, Japan

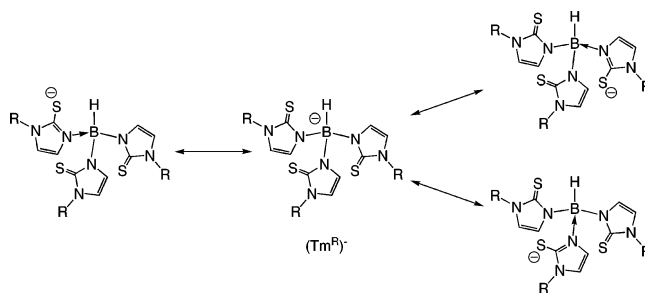
Received June 7, 2006

A series of $[\text{Tm}^{\text{Me}}\text{M}(\mu\text{-Cl})_2]$ and $\text{Tm}^{\text{R}}\text{MCl}$ (Tm^{R} = tris(mercaptoimidazolyl)borate; R = Me, ^tBu, Ph, 2,6-ⁱPr₂C₆H₃ (Ar); M = Mn, Fe, Co, Ni) complexes have been prepared by treatment of NaTm^{Me} or LiTm^{R} with an excess amount of metal(II) chlorides, MCl_2 . Treatment of $\text{Tm}^{\text{R}}\text{MCl}$ (R = ^tBu, Ph, Ar) with NaI led to a halide exchange to afford $\text{Tm}^{\text{R}}\text{MI}$. The molecular structures of $[\text{Tm}^{\text{Me}}\text{M}(\mu\text{-Cl})_2]$ (M = Mn, Ni), $[\text{Tm}^{\text{Me}}\text{Ni}(\mu\text{-Br})_2]$, $\text{Tm}^{\text{Bu}}\text{MCl}$ (M = Fe, Co), $\text{Tm}^{\text{Ph}}\text{MCl}$ (M = Mn, Fe, Co, Ni), $\text{Tm}^{\text{Ar}}\text{MCl}$ (M = Mn, Fe, Co, Ni), $\text{Tm}^{\text{Ph}}\text{MI}$ (M = Mn, Co), and $\text{Tm}^{\text{Ar}}\text{MI}$ (M = Fe, Co, Ni) have been determined by X-ray crystallography. The Tm^{R} ligands occupy the tripodal coordination site of the metal ions, giving a square pyramidal or trigonal bipyramidal coordination geometry for $[\text{Tm}^{\text{Me}}\text{M}(\mu\text{-Cl})_2]$ and a tetrahedral geometry for the $\text{Tm}^{\text{R}}\text{MCl}$ complexes, where the S–M–S bite angles are larger than the reported N–M–N angles of the corresponding hydrotris(pyrazolyl)borate (Tp^{R}) complexes. Treatment of $\text{Tm}^{\text{Ph}}_2\text{Fe}$ with excess FeCl_2 affords $\text{Tm}^{\text{Ph}}\text{FeCl}$, indicating that $\text{Tm}^{\text{R}}_2\text{M}$ as well as $\text{Tm}^{\text{R}}\text{MCl}$ is formed at the initial stage of the reaction between MCl_2 and the Tm^{R} anion.

Introduction

Tripodal face-capping ligands have proven to be useful entities for transition metal chemistry. The most well-known type of such ligands is hydrotris(pyrazolyl)borate and its derivatives (Tp^{R}) with a wide variety of substitutions (R) on the pyrazole rings;¹ the coordination chemistry of Tp^{R} has been extensively explored. The related borate ligands, including (thioether)borates $\text{PhB}(\text{CH}_2\text{SR})_3$ ² and (phosphino)borates $\text{PhB}(\text{CH}_2\text{PR}_2)_3$,³ have also been explored for a range of late transition metal complexes. The advantages of these

ligands are their negatively charged properties, leading to a stable coordination to the metal ions, as well as their varied steric influence at the metals according to the size of the substituents on the ligands. Recently, hydrotris(mercaptoimidazolyl)borates (Tm^{R}), a new class of such tripodal borate



ligands, has been developed by Reglinski and co-workers.⁴ An important property of the Tm^{R} ligands is the delocalized anionic charge on the thioimidazole groups, which brings about the thiolate-like character of the thioimidazole sulfurs.

* To whom correspondence should be addressed. E-mail: i45100a@nucc.cc.nagoya-u.ac.jp. Fax: +81-52-789-2943.

[†] Present address: Coordination Chemistry Laboratory, Institute for Molecular Science, Myodaiji, Okazaki 444-8595, Japan.

- (1) (a) Chaudhuri, P.; Wieghardt, K. *Prog. Inorg. Chem.* **1987**, *35*, 329. (b) Cooper, S. P. *Acc. Chem. Res.* **1988**, *21*, 141. (c) Trofimenko, S. *Chem. Rev.* **1993**, *93*, 943. (d) Trofimenko, S. *Scorpionates*; Imperial College Press: London, 1999.
- (2) (a) Ge, P.; Haggerty, B. S.; Rheingold, A. L.; Riordan, C. G. *J. Am. Chem. Soc.* **1994**, *116*, 8406. (b) Ohrenberg, C.; Ge, P.; Schebler, P. J.; Riordan, C. G.; Yap, G. P. A.; Rheingold, A. L. *Inorg. Chem.* **1996**, *35*, 749. (c) Ohrenberg, C.; Saleem, M. M.; Riordan, C. G.; Yap, G. P. A.; Rheingold, A. L. *Chem. Commun.* **1996**, 1081. (d) Schebler, P. J.; Riordan, C. G.; Liable-Sands, L.; Rheingold, A. L. *Inorg. Chim. Acta* **1998**, *270*, 543. (e) Schebler, P. J.; Riordan, C. G.; Guzei, I. A.; Rheingold, A. L. *Inorg. Chem.* **1998**, *37*, 4754. (f) Ohrenberg, C.; Riordan, C. G.; Liable-Sands, L.; Rheingold, A. L. *Coord. Chem. Rev.* **1998**, *174*, 301.

- (3) (a) Barney, A. A.; Heyduk, A. F.; Nocera, D. G. *Chem. Commun.* **1999**, 2379. (b) Peters, J. C.; Feldman, J. D.; Tilly, T. D. *J. Am. Chem. Soc.* **1999**, *121*, 9871. (c) Betley, T. A.; Peters, J. C. *Inorg. Chem.* **2003**, *42*, 5074.

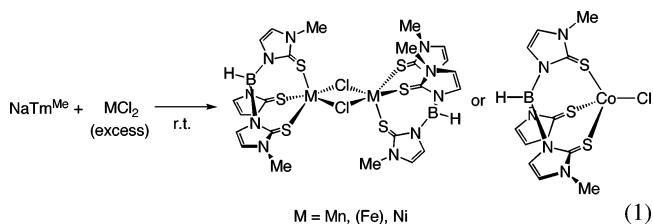
One notable aspect of these face-capping ligands is their application to the models of the metal-containing enzymes. Various model complexes of metalloenzyme active sites coordinated by histidine imidazoles such as hemerythrin and hemocyanin have been accomplished by utilization of Tp^{R} ligands.⁵ Sulfur-ligated transition metal centers are also abundant in enzymes such as nitrogenase, hydrogenase, and carbon monoxide dehydrogenase, and the modeling of these active sites has been the focus of our attention.⁶ In terms of mimicking the active site of metalloenzymes bearing sulfur ligands, tripodal sulfur ligands have also been used. For instance, several $\text{Tm}^{\text{R}}\text{Zn}$ complexes were prepared to mimic the sulfur-rich environments of zinc enzymes featuring a tetrahedral coordination in the Ada repair protein or liver alcohol dehydrogenase (LADH).⁷

The chemistry of the Tm^{C} -metal complexes is potentially rich and important because analogous structural types observed with Tp^{R} ligands would be available with Tm^{R} ligands and the substituents on the imidazole rings are suitable for steric modification. As the tetrahedral transition metal halide complexes of the Tp^{R} derivatives, $\text{Tp}^{\text{R}}\text{MCl}$,⁸ are known to be versatile precursors for a wide range of transition metal mono- Tp^{R} complexes, the analogous compounds comprising a Tm^{R} ligand, $\text{Tm}^{\text{R}}\text{MX}$ ($\text{X} = \text{halides}$), are also expected to be useful synthons. However, such types of Tm^{R} -transition metal complexes are still rare, probably because of their propensity to form sandwich complexes $(\text{Tm}^{\text{R}})_2\text{M}$.^{9,10} Whereas efficient synthetic procedures for cobalt complexes, $\text{Tm}^{\text{R}}\text{CoX}$ ($\text{R} = \text{Me}, \text{tBu}; \text{X} = \text{Cl}, \text{Br}, \text{I}$), have recently appeared,⁹ we found a convenient route to the $\text{M}(\text{II})$ ($\text{M} = \text{Mn}, \text{Fe}, \text{Co}, \text{Ni}$) halide complexes with a Tm^{R} ligand using metal halides and the alkaline metal salts of

Tm^{R} . In contrast to the previous reports that discussed the formation of $(\text{Tm}^{\text{R}})_2\text{M}$ by the reaction of MCl_2 and the Tm^{R} anion in a 1:1 molar ratio, $\text{Tm}^{\text{R}}\text{MCl}$ complexes were obtained selectively by addition of excess MCl_2 to the Tm^{R} anion. The use of excess MCl_2 toward the Tm^{R} anion and the prolonged reaction time turned out to be the keys for the successful formation of the anticipated $\text{Tm}^{\text{R}}\text{MX}$ complexes. We report herein the preparation of the mono- Tm^{R} ($\text{R} = \text{Me}, \text{tBu}, \text{Ph}, \text{Ar}; \text{Ar} = 2,6\text{-iPr}_2\text{C}_6\text{H}_3$) complexes of metal halides, $[\text{Tm}^{\text{Me}}\text{M}(\mu\text{-Cl})_2]$ and $\text{Tm}^{\text{R}}\text{MX}$ ($\text{M} = \text{Mn}, \text{Fe}, \text{Co}, \text{Ni}; \text{X} = \text{Cl}, \text{I}$), which would be useful starting materials for various transition metal complexes of Tm^{R} .

Results and Discussion

Synthesis of $\text{Tm}^{\text{R}}\text{MX}$ and $[\text{Tm}^{\text{Me}}\text{M}(\mu\text{-X})_2]$ Complexes ($\text{R} = \text{Me}, \text{tBu}, \text{Ph}, 2,6\text{-iPr}_2\text{C}_6\text{H}_3(\text{Ar}); \text{M} = \text{Mn}, \text{Fe}, \text{Co}, \text{Ni}; \text{X} = \text{Cl}, \text{I}$). In order to synthesize the target compounds, we first attempted the reaction of FeCl_2 with 1 equiv of NaTm^{Me} or LiTm^{Ph} . However, these reactions appeared to give the sandwich-type complex $\text{Tm}^{\text{R}}_2\text{Fe}$. Indeed, Reglinski, Parkin, and their co-workers have already demonstrated that the reactions of $\text{M}'\text{Cl}_2$ ($\text{M}' = \text{Fe}, \text{Ni}$) with NaTm^{Me} or $\text{M}''\text{Cl}_2$ ($\text{M}'' = \text{Fe}, \text{Co}$) with LiTm^{Ph} afford $\text{Tm}^{\text{Me}}_2\text{M}'$ ($\text{M}' = \text{Fe}, \text{Ni}$) or $\text{Tm}^{\text{Ph}}_2\text{M}''$ ($\text{M}'' = \text{Fe}, \text{Co}$), respectively.^{10,11} The dominant formation of sandwich complexes would be attributed to the much lower solubility of FeCl_2 than that of the mono- Tm^{R} -substituted complexes. That is, during the course of the reactions, the concentration of the mono- Tm^{R} complexes is expected to exceed that of FeCl_2 , which leads to the more preferable formation of the sandwich complexes. However, we found that the prolonged reaction time in the presence of excess FeCl_2 allows the selective formation of the mono- Tm^{R} -substituted complexes. Treatment of the LiTm^{Ph} with excess FeCl_2 at room temperature in dichloromethane immediately afforded a dark green suspension, which indicated the formation of $\text{Tm}^{\text{R}}_2\text{Fe}$. However, over the course of the reaction for 4 days, the dark green color gradually became brighter, and eventually, the green suspension was obtained. The monocuclear $\text{Tm}^{\text{Ph}}\text{FeCl}$ complex was obtained in 86% yield after the usual workup.



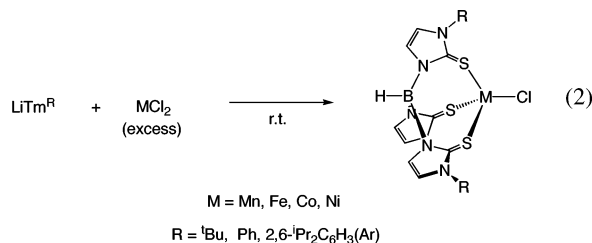
A similar reaction with LiTm^{tBu} and NaTm^{Me} also led to the formation of the mono- Tm^{tBu} - and mono- Tm^{Me} -substi-

- (4) (a) Garner, M.; Reglinski, J.; Cassidy, I.; Spicer, M. D.; Kennedy, A. R. *Chem. Commun.* **1996**, 1975. (b) Reglinski, J.; Garner, M.; Cassidy, I. D.; Slavin, P. A.; Spicer, M. D.; Armstrong, D. R. *J. Chem. Soc., Dalton Trans.* **1999**, 2119.
- (5) (a) Armstrong, W. H.; Lippard, S. J. *J. Am. Chem. Soc.* **1987**, *109*, 4837. (b) Kitajima, N.; Fujisawa, K.; Fujimoto, C.; Moro-oka, Y.; Hashimoto, S.; Kitagawa, T.; Toriumi, K.; Tatsumi, K.; Nakamura, A. *J. Am. Chem. Soc.* **1992**, *114*, 1277. (c) Kitajima, N.; Moro-oka, Y. *Chem. Rev.* **1994**, *94*, 737. (d) Feig, A. L.; Lippard, S. J. *Chem. Rev.* **1994**, *94*, 759.
- (6) (a) Ohki, Y.; Sunada, Y.; Honda, M.; Katada, M.; Tatsumi, K. *J. Am. Chem. Soc.* **2003**, *125*, 4052. (b) Ohki, Y.; Sunada, Y.; Tatsumi, K. *Chem. Lett.* **2005**, *34*, 172. (c) Li, Z.; Ohki, Y.; Tatsumi, K. *J. Am. Chem. Soc.* **2005**, *127*, 8950. (d) Takuma, M.; Ohki, Y.; Tatsumi, K. *Inorg. Chem.* **2005**, *44*, 6034. (e) Takuma, M.; Ohki, Y.; Tatsumi, K. *Organometallics* **2005**, *24*, 1344.
- (7) (a) Kimblin, C.; Bridgewater, B. M.; Churchill, D. G.; Parkin, G. *Chem. Commun.* **1999**, 2301. (b) Parkin, G. *Chem. Commun.* **2000**, 1971. (c) Bridgewater, B. M.; Fillebeen, T.; Friesner, R. A.; Parkin, G. *J. Chem. Soc., Dalton Trans.* **2000**, 4494. (d) Tesmer, M.; Shu, M.; Vahrenkamp, H. *Inorg. Chem.* **2001**, *40*, 4022.
- (8) (a) Trofimenko, S. *Prog. Inorg. Chem.* **1986**, *34*, 115. (b) Gorrell, I. B.; Parkin, G. *Inorg. Chem.* **1990**, *29*, 2452. (c) LeCloux, D. D.; Keyes, M. C.; Osawa, M.; Reynolds, V.; Tolman, W. B. *Inorg. Chem.* **1994**, *33*, 6361. (d) Huang, J.; Lee, L.; Haggerty, B. S.; Rheingold, A. L.; Walters, M. A. *Inorg. Chem.* **1995**, *34*, 4268. (e) Kremer, -A. A.; Klauui, W.; Bell, R.; Strerath, A.; Wunderlich, H.; Mootz, D. *Inorg. Chem.* **1997**, *36*, 1552. (f) Kisko, J. L.; Hascall, T.; Parkin, G. *J. Am. Chem. Soc.* **1998**, *120*, 10561. (g) Guo, S.; Ding, E.; Yin, Y.; Yu, K. *Polyhedron* **1998**, *17*, 3841. (h) Chen, J.; Woo, L. K. *J. Organomet. Chem.* **2000**, *601*, 57. (i) Brunker, T. J.; Hascall, T.; Cowley, A. R.; Rees, L. H.; O'Hare, D. *Inorg. Chem.* **2001**, *40*, 3170. (j) Rheingold, A. L.; Yap, G. P. A.; Zakharov, L. N.; Lev, N.; Trofimenko, S. *Eur. J. Inorg. Chem.* **2002**, *9*, 2335. (k) Trofimenko, S.; Rheingold, A. L.; Sands, L. M. L. *Inorg. Chem.* **2002**, *41*, 1889.

- (9) (a) Mihalcic, D. J.; White, J. L.; Tanski, J. M.; Zakharov, L. N.; Yap, G. P. A.; Incarvito, C. D.; Rheingold, A. L.; Rabinovich, D. *J. Chem. Soc., Dalton Trans.* **2004**, 1626. (b) Dodds, C. A.; Lehmann, M.-A.; Ojo, J. F.; Reglinski, J.; Spicer, M. D. *Inorg. Chem.* **2004**, *43*, 4927.
- (10) Kimblin, C.; Churchill, D. G.; Bridgewater, B. M.; Girard, J. N.; Quarless, D. A.; Parkin, G. *Polyhedron* **2001**, *20*, 1891.
- (11) Garner, M.; Lewinski, K.; Patek-Janczyk, A.; Reglinski, J.; Sieklucka, B.; Spicer, M. D.; Szalaniec, M. *J. Chem. Soc., Dalton Trans.* **2003**, 1181.

tuted complexes, respectively. The molecular structures of $\text{Tm}^{\text{Ph}}\text{FeCl}$ and $\text{Tm}^{\text{tBu}}\text{FeCl}$ were eventually determined by X-ray structural analysis, and their monomeric structures were identified (*vide infra*). However, the nuclearity of the product having less hindered Tm^{Me} in the solid state was not yet identified as $\text{Tm}^{\text{Ph}}\text{FeCl}$ or $[\text{Tm}^{\text{Me}}\text{Fe}(\mu\text{-Cl})]_2$ due to the lack of the solid-state structure. The fast atom bombardment mass spectrometry (FABMS) spectrum of $(\text{Tm}^{\text{Me}}\text{FeCl})_n$ ($n = 1$ or 2) in CH_2Cl_2 exhibited a characteristic signal, the isotope pattern of which matches well with that calculated for $[\text{Tm}^{\text{Me}}\text{Fe}]^+$ ($m/z = 406.9$). Whereas this indicates the formation of the monomeric complex $\text{Tm}^{\text{Me}}\text{FeCl}$ in solution, we presume this $\text{Tm}^{\text{Me}}\text{Fe}$ complex to be the dimeric structure in the solid state because the color of the CH_2Cl_2 solution (deep green) is different from that in the solid state (green). Such a color change is also found for the dimeric nickel complex $[\text{Tm}^{\text{Me}}\text{Ni}(\mu\text{-Cl})]_2$, as described below.

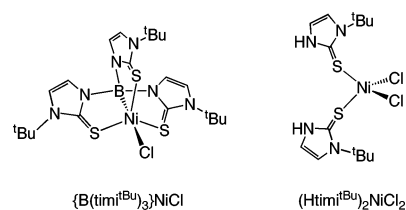
The yields of $\text{Tm}^{\text{R}}\text{FeCl}$ (or $[\text{Tm}^{\text{Me}}\text{Fe}(\mu\text{-Cl})]_2$) are typically higher than 80% based on the Tm^{R} anions (25% and above, based on FeCl_2). They are moderately stable toward air and moisture in the solid state, but unstable in solution. Regardless of the substituents on the imidazole rings, products are soluble in dichloromethane and THF, but sparingly soluble in toluene, ether, and hexane. The color of the product dramatically varies according to the substituents on the Tm^{R} ligands. For instance, $\text{Tm}^{\text{tBu}}\text{FeCl}$ is light brown, $\text{Tm}^{\text{Ph}}\text{FeCl}$ is dark green, and $\text{Tm}^{\text{Ar}}\text{FeCl}$ is dark yellow. It seems likely that the substituent on the thioimidazolyl unit modifies the electron-donating ability. The representation of the tetrahedral $\text{Tm}^{\text{R}}\text{FeCl}$ closely parallels the Tp complexes and may thus provide an entry to various derivatives analogous to the Tp chemistry.



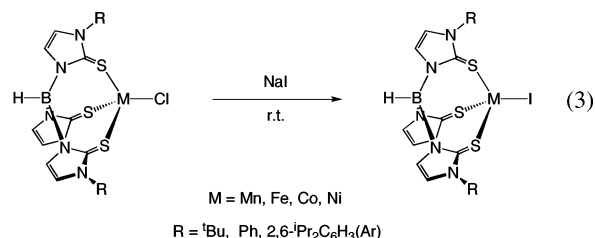
The cobalt and nickel complexes, $\text{Tm}^{\text{R}}\text{CoCl}$ and $\text{Tm}^{\text{R}}\text{NiCl}$, were also synthesized by a similar procedure, whereas the preparation of $\text{Tm}^{\text{R}}\text{MnCl}$ was achieved by a 1:1 reaction between MnCl_2 and the Tm^{R} anion in methanol. All manganese complexes are colorless, but the colors of the cobalt and nickel complexes change because of the substituents on the mercaptoimidazolyl group, for instance, $\text{Tm}^{\text{tBu}}\text{CoCl}$ (green), $\text{Tm}^{\text{Ar}}\text{CoCl}$ (light blue), $\text{Tm}^{\text{Ph}}\text{NiCl}$ (green), and $\text{Tm}^{\text{Ar}}\text{NiCl}$ (greenish brown). The Tm^{Me} complexes of Mn and Ni were isolated as the dimeric form, $[\text{Tm}^{\text{Me}}\text{M}(\mu\text{-Cl})]_2$ ($M = \text{Mn, Ni}$). The bulkiness of the substituent on the imidazole ring likely results in the difference in nuclearity, whereas the analogous cobalt(II) complex $\text{Tm}^{\text{Me}}\text{CoCl}$ is reported to be monomeric.^{9b} The yields for the Mn, Co, and Ni complexes are satisfactory and typically higher than 50% based on the added Tm^{R} anions (89–12% based on MCl_2), with exceptions for the Tm^{Me} and Tm^{tBu} complexes of nickel.

The yield of $[\text{Tm}^{\text{Me}}\text{Ni}(\mu\text{-Cl})]_2$ was very low due to the dominant formation of the sandwich complex $\text{Tm}^{\text{Me}}\text{Ni}_2$,¹⁰ which precipitates out from the reaction mixture. In contrast, $[\text{Tm}^{\text{Me}}\text{Ni}(\mu\text{-Br})]_2$ was obtained in 71% yield (based on NaTm^{Me}) by a similar procedure using NiBr_2 instead of NiCl_2 . In the mass spectra, all the $[\text{Tm}^{\text{Me}}\text{M}(\mu\text{-Cl})]_2$ and $\text{Tm}^{\text{R}}\text{-MCl}$ complexes exhibited cationic signals corresponding to the $[\text{Tm}^{\text{R}}\text{M}]^+$ species. The monomeric form $\text{Tm}^{\text{Me}}\text{MCl}$ is presumably generated in solution for the dimeric complexes $[\text{Tm}^{\text{Me}}\text{M}(\mu\text{-Cl})]_2$. Indeed, the solution color for $[\text{Tm}^{\text{Me}}\text{Ni}(\mu\text{-Cl})]_2$ (deep green) differs from that in the solid state (green).

The reaction of NiCl_2 with the Tm^{tBu} anion did not afford the corresponding adduct but instead a nickelaboratrane complex of Ni(I), $\{\text{B}(\text{tmi}^{\text{tBu}})_3\}\text{NiCl}$. During the formation



of the nickelaboratrane complex, activation of the B–H bond accompanied by formal reduction of the metal center to Ni(I) took place to give a five-coordinate complex having a direct Ni–B dative bond. This is the first nickelaboratrane complex, whereas the related metallaboratrane complexes of Ru, Os, Co, Ir, Rh, and Pt have recently been synthesized by Hill and Rabinovich.^{9a,12} A small amount of the *tert*-butylthioimidazole (Htmi^{tBu}) complex, $(\text{Htmi}^{\text{tBu}})_2\text{NiCl}_2$, was also isolated as well from this reaction, which probably came from the degraded Tm^{tBu} anion prior to use. Indeed, $(\text{Htmi}^{\text{tBu}})_2\text{NiCl}_2$ was alternatively prepared in 75% yield by the reaction of NiCl_2 with 2 equiv of Htmi^{tBu} .



Treatment of monomeric $\text{Tm}^{\text{R}}\text{MCl}$ with NaI provided an excellent preparative route to the corresponding iodide analogues, $\text{Tm}^{\text{R}}\text{MI}$, whereas the reaction of MI_2 with the alkaline metal salt of Tm^{R} affords multiple products that could not be separated. The halide exchange successfully proceeded for the mononuclear, tetrahedral complexes $\text{Tm}^{\text{R}}\text{-}$

- (12) (a) Hill, A. F.; Owen, G. R.; White, A. J. P.; Williams, D. J. *Angew. Chem., Int. Ed.* **1999**, *38*, 2759. (b) Foreman, M. R. St. -J.; Hill, A. F.; Owen, G. R.; White, A. J. P.; Williams, D. J. *Organometallics* **2003**, *22*, 4446. (c) Foreman, M. R. St. -J.; Hill, A. F.; White, A. J. P.; Williams, D. J. *Organometallics* **2004**, *23*, 913. (d) Crossley, I. R.; Hill, A. F. *Organometallics* **2004**, *23*, 5656. (e) Crossley, I. R.; Hill, A. F.; Willis, A. C. *Organometallics* **2005**, *24*, 1062. (f) Crossley, I. R.; Foreman, M. R. St. -J.; Hill, A. F.; White, A. J. P.; Williams, D. J. *Chem. Commun.* **2005**, 221. (g) Crossley, I. R.; Hill, A. F.; Humphrey, E. R.; Willis, A. C. *Organometallics* **2005**, *24*, 4083. (h) Crossley, I. R.; Hill, A. F.; Willis, A. C. *Organometallics* **2006**, *23*, 289.

Table 1. Properties and Spectral Data for Complexes

compound	color	yield based on [Tm ^R] ⁻ (based on MCl ₂) ^a	IR (B–H) ^a	UV–vis (ε) ^a	mass spectrum (CH ₂ Cl ₂) ^b
Tm ^{Me} FeCl	green	78 (26)	2438	264 (18.6), 306 (6.9, sh), 406 (2.9), 614 (1.3)	406.9 ([M] ⁺ – Cl)
Tm ^{iBu} FeCl	light brown	94 (94)	2408	276 (1.0), 357 (0.26, sh), 421 (0.08, sh)	568.2 ([M], 10%), 533.1 ([M] ⁺ – Cl, 100%)
Tm ^{Ph} FeCl	dark green	86 (86)	2431	361 (1.7, sh), 446 (0.93, sh), 646 (0.69)	593.1 ([M] ⁺ – Cl)
Tm ^{Ar} FeCl	brown	99 (25)	2409	285 (1.5, sh), 345 (0.32, sh)	880.5 ([M], 80%), 845.5 ([M] ⁺ – Cl, 100%)
[Tm ^{Me} Mn(μ-Cl)] ₂	colorless	54 (54)	2391	261 (27.2)	406.5 (1/2[M] ⁺ – Cl)
Tm ^{iBu} MnCl	colorless	89 (89)	2411	269 (22.0)	532.1 ([M] ⁺ – Cl)
Tm ^{Ph} MnCl	colorless	35 (35)	2420	280 (16.7)	592.2 ([M] ⁺ – Cl)
Tm ^{Ar} MnCl	colorless	86 (86)	2413	271 (28.6)	844.5 ([M] ⁺ – Cl)
Tm ^{Me} CoCl	green	37 (12)	2410	371 (4.2), 697 (1.2)	410.1 ([M] ⁺ – Cl)
Tm ^{iBu} CoCl	green	77 (77)	2410	369 (3.4), 665 (0.96), 701 (1.3), 738 (1.0)	563.3 ([M] ⁺ – Cl)
Tm ^{Ph} CoCl	green	59 (20)	2418	279 (7.9), 371 (2.2), 663 (0.64), 702 (0.85), 740 (0.63)	596.2 ([M] ⁺ – Cl)
Tm ^{Ar} CoCl	light blue	55 (18)	2440	369 (0.35), 665 (0.09), 701 (0.14), 738 (0.10)	848.5 ([M] ⁺ – Cl)
[Tm ^{Me} Ni(μ-Cl)] ₂	green	18 (3.5)	2387	267 (12.5), 331 (4.6), 378 (4.3), 424 (4.2)	409.1 (1/2[M] ⁺ – Cl)
[Tm ^{Me} Ni(μ-Br)] ₂	brown	71 (71)	2440	330 (7.6), 363 (7.1, sh), 426 (6.7, sh), 731 (4.6, sh)	409.1 (1/2[M] ⁺ – Br)
Tm ^{Ph} NiCl	green	55 (19)	2431	392 (3.9), 640 (0.45), 730 (0.38, sh)	595.2 ([M] ⁺ – Cl)
Tm ^{Ar} NiCl	yellowish green	79 (20)	2439	284 (2.6), 384 (0.67), 450 (0.19, sh)	882.4 ([M] ⁺ , 10%), 847.4 ([M] ⁺ – Cl, 100%)
Tm ^{iBu} FeI	brown	93 ^c	2424	286 (29.5), 361 (10.7)	534.3 ([M] ⁺ – I)
Tm ^{Ph} FeI	green	64 ^c	2431	290 (16.9), 446 (4.8, sh), 646 (2.1)	593.2 ([M] ⁺ – I)
Tm ^{Ar} FeI	yellow	55 ^c	2424	341 (4.1)	845.4 ([M] ⁺ – I)
Tm ^{iBu} MnI	colorless	95 ^c	2414	274 (19.4)	532.3 ([M] ⁺ – I)
Tm ^{Ph} MnI	colorless	93 ^c	2422	278 (13.2)	592.2 ([M] ⁺ – I)
Tm ^{Ar} MnI	colorless	76 ^c	2435	275 (28.5)	844.5 ([M] ⁺ – I)
Tm ^{iBu} CoI	light yellow	93 ^c	2411	393 (2.5, sh), 695 (0.78), 740 (0.91, sh), 758 (0.98)	536.3 ([M] ⁺ – I)
Tm ^{Ph} CoI	green	46 ^c	2436	393 (2.5, sh), 694 (0.65), 730 (0.86), 761 (1.0)	596.2 ([M] ⁺ – I)
Tm ^{Ar} CoI	yellow	75 ^c	2436	269 (17.2), 406 (0.92), 759 (0.11)	848.5 ([M] ⁺ – I)
Tm ^{Ph} NiI	orange	86 ^c	2413	411 (4.8), 699 (0.45), 784 (0.35, sh)	595.2 ([M] ⁺ – I)
Tm ^{Ar} NiI	orange	69 ^c	2435	273 (32.2), 402 (4.8)	848.5 ([M] ⁺ – I)
{B(timi ^{iBu}) ₃ }NiCl	green	69 (69)		342 (4.0), 459 (1.9), 612 (0.40)	534.2 ([M] ⁺ – Cl)

^a Yields, %, IR, cm⁻¹. λ_{max}, nm (ε, × 10³ M⁻¹cm⁻¹), in CH₂Cl₂, rt. ^b FABMS (*m/z*) with a stream of high energy Xe gas. 3-Nitrobenzyl alcohol was used as the matrix. ^c Yields based on the corresponding Tm^RMCl.

MCl (R = ⁱBu, Ph, Ar, M = Fe, Mn, Co, Ni) having a terminal chloride but did not occur for the Tm^{Me} complexes [Tm^{Me}M(μ-Cl)]₂ (M = Mn, Ni). The exchange of the halide also led to a color change for the Fe, Co, and Ni compounds. For instance, Tm^{Ph}NiX is green for X = Cl and orange for X = I.

In the IR spectra, the Tm^RMX complexes exhibited characteristic bands for the Tm^R ligand, ν(B–H), as summarized in Table 1. The range for the B–H band (2387–2440 cm⁻¹) is similar to that for the κ³-Tp complexes,¹ indicating that B–H–M interactions do not exist. A slight shift of the ν(B–H) band to a lower frequency was found from 2478 cm⁻¹ for NaTm^{Me} to 2387–2438 cm⁻¹ for [Tm^{Me}M(μ-Cl)]₂ and 2409–2440 cm⁻¹ for Tm^RMX. This can be attributed to the enhancement of the anionic charge at the coordinated sulfur atoms, which reduces the negative charge at B–H.

Structures of the Tm^RMX Complexes. The X-ray structure analyses were carried out for [Tm^{Me}M(μ-Cl)]₂ (M = Mn, Ni), [Tm^{Me}Ni(μ-Br)]₂, Tm^{iBu}MCl (M = Fe, Co), Tm^{Ph}-MCl (M = Mn, Fe, Co, Ni), Tm^{Ar}MCl (M = Mn, Fe, Co, Ni), Tm^{iBu}FeI, Tm^{Ph}MI (M = Mn, Co, Ni), and Tm^{Ar}MI (M =

Fe, Co, Ni). Because the molecular structures of the Mn, Fe, Co, Ni complexes are very similar, the perspective views of only one of each Tm^R complex are shown in Figure 1, and the selected bond lengths and angles are listed in Tables 2 and 3, respectively. In the case of Tm^{Me}, a dimeric structure featuring a trigonal bipyramidal (Mn) or square pyramidal (Ni) geometry is formed with an inversion center at the midpoint between the two metals. The shorter axial Ni–S distance (2.3212(8) Å for the Cl complex) than the basal Ni–S distances (2.4026(8) and 2.3468(8) Å for Cl complex) is typical for square pyramidal complexes. The shorter metal–sulfur distance also leads to the longer S=C bond as a result of the back-donation from the metal to the thioimidazol group. This is also the case for the trigonal bipyramidal Mn complex, with longer Mn–S(axial)/C=S(equatorial) and shorter Mn–S(equatorial)/C=S(axial) bonds. The other Tm^R (R = ⁱBu, Ph, Ar) complexes adopt a mononuclear tetrahedral geometry having an ideal C₃ axis running through the B, M, and X atoms. All the Tm^R ligands are bound to metals in a κ³-fashion, forming eight-membered metallacycles consisting of the metal, two mercaptoimidazolyl groups, and boron. This leads to larger S–M–S bite angles (around 105° for Tm^R-

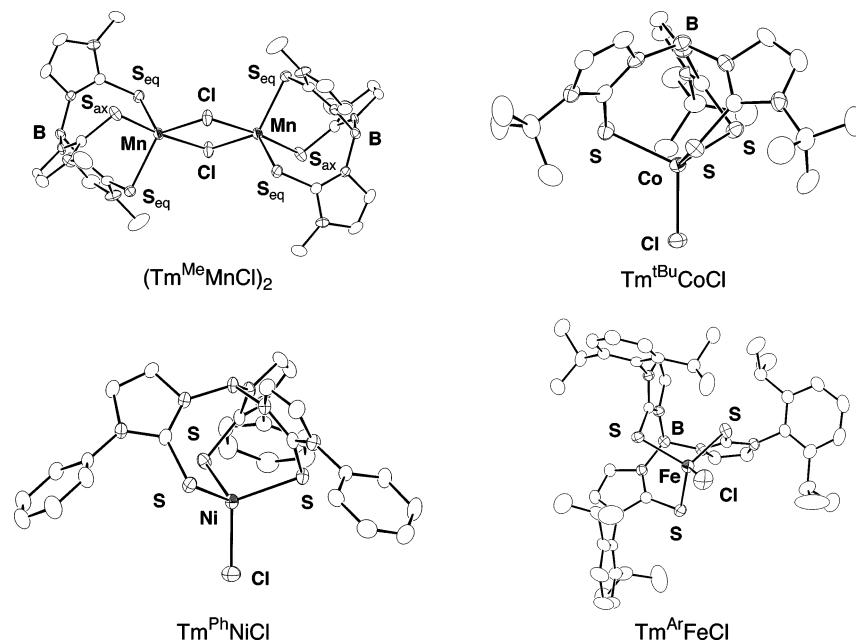


Figure 1. Molecular structures of $[\text{Tm}^{\text{Me}}\text{Mn}(\mu\text{-Cl})_2]$ (top, left), $\text{Tm}^{\text{tBu}}\text{CoCl}$ (top, right), $\text{Tm}^{\text{Ph}}\text{NiCl}$ (bottom, left), and $\text{Tm}^{\text{Ar}}\text{FeCl}$ (bottom, right).

Table 2. Selected Bond Distances (Å) for the Dinuclear Complexes $[\text{Tm}^{\text{Me}}\text{Mn}(\mu\text{-Cl})_2]$, $[\text{Tm}^{\text{Me}}\text{Ni}(\mu\text{-Cl})_2]$, and $[\text{Tm}^{\text{Me}}\text{Ni}(\mu\text{-Br})_2]$

	M–S (ax.), M–S (eq or basal)	M–Cl (Br)	C=S (ax.), C=S (eq or basal)
$(\text{Tm}^{\text{Me}}\text{MnCl})_2$	2.5698(6), 2.477(av)	2.4149(6)	1.707(2), 1.719 (av)
$(\text{Tm}^{\text{Me}}\text{NiCl})_2$	2.3212(8), 2.3747 (av)	2.3818(9), 2.4129(7)	1.723(3), 1.720 (av)
$(\text{Tm}^{\text{Me}}\text{NiBr})_2$	2.3116(6), 2.3665 (av)	2.5192(4), 2.5684(4)	1.722(3), 1.717 (av)

Table 3. Selected Bond Distances (Å) and Angles (deg) for Monomeric $\text{Tm}^{\text{R}}\text{MX}$ (R = ^tBu, Ph; Ar = 2,6-ⁱPr₂C₆H₃; M = Mn, Fe, Co, Ni; X = Cl, I)

M	X	R	M–S	M–X	C=S	S–M–S	S–M–X
Mn	Cl	Ph	2.454(2)	2.326(2)	1.719(4)	103.53(5)	114.91(4)
Mn	Cl	Ar	2.435(3)	2.295(4)	1.710(9)	105.43(8)	113.26(7)
Fe	Cl	Ph	2.385(1)	2.255(3)	1.713(5)	104.76(4)	113.85(4)
Fe	Cl	Ar	2.3798 (av)	2.2381(6)	1.712 (av)	104.91 (av)	113.70 (av)
Co	Cl	^t Bu	2.3331(7)	2.220(2)	1.723(4)	105.26(3)	113.41(2)
Co	Cl	Ph	2.327(1)	2.252(2)	1.715(4)	107.42(4)	111.45(4)
Co	Cl	Ar	2.312(1)	2.242(2)	1.705(3)	108.22(3)	110.70(3)
Ni	Cl	Ph	2.3000(7)	2.235(1)	1.716(3)	104.47(3)	114.10(2)
Ni	Cl	Ar	2.2866(8)	2.216(1)	1.712(3)	105.14(2)	113.51(2)
Mn	I	Ph	2.437(2)	2.626(2)	1.707(6)	104.38(6)	114.18(5)
Fe	I	Ar	2.366 (av)	2.556(1)	1.711 (av)	106.22 (av)	112.53 (av)
Co	I	Ph	2.3071(9)	2.5789(9)	1.725(3)	108.55(3)	110.38(3)
Co	I	Ar	2.298(1)	2.542(1)	1.714(4)	109.57(3)	109.38(3)
Ni	I	Ar	2.2847 (av)	2.515 (av)	1.712 (av)	105.25 (av)	113.32 (av)
Fe	Cl	^t Bu	2.3883(7)	2.232(1)	1.730(2)	102.69(2)	115.61(2)
Fe	I	^t Bu	2.370(1)	2.573(1)	1.731(4)	104.27(5)	114.28(4)
Ni	I	Ph	2.2780(9)	2.545(1)	1.710(4)	105.08(4)	113.57(3)

MCl) than the N–M–N angles for the six-membered metallacycles in the Tp complexes (ca. 90°). A larger S–M–S bite angle steers the substituents on Tm^{R} toward the metal center, and this facilitates the formation of mono- Tm complexes. Indeed, the reaction of MCl_2 with the Tm^{Me} anion can afford the chloride-bridged dimer $[\text{Tm}^{\text{Me}}\text{M}(\mu\text{-Cl})_2]$ or monomeric $\text{Tm}^{\text{Me}}\text{CoCl}$, whereas the Tp^{Me} analogue is not available. The M–S and M–Cl distances follow the order of the ion radii, $\text{Mn} > \text{Fe} > \text{Co} > \text{Ni}$. Although $\text{Tm}^{\text{R}}\text{MCl}$ and $[\text{Tm}^{\text{Me}}\text{M}(\mu\text{-Cl})_2]$ complexes comprise various numbers of d-electrons ranging from d^5 Mn(II) to d^8 Ni(II), there is no notable difference in the C=S distances. Similarly, the exchange of the halogen or the Tm^{R} substituents has almost no influence on these bonds. These results indicate that the

back-donation from the metal to the thioimidazol group is not significant during the interaction between the metals and the Tm^{R} ligands, and thus ligation of the C=S group is expected to be labile.

Structure of the Nickelaboratarane Complex. The molecular geometry of $\{\text{B}(\text{timi}^{\text{tBu}})_3\}\text{NiCl}$ is illustrated in Figure 2, which exhibits a trigonal bipyramidal arrangement around the nickel with a direct Ni–B bond (2.108(4) Å). The nickel–boron linkage is compared with those observed in the metallaboratarane complexes of Ru, Os, Co, Rh, and Ir,^{9a,12} the most closely aligned example of which is the cobaltaboratarane complex (Co–B, 2.132(4) Å).^{9a} The boron atom is tetrahedrally coordinated with angles in the range of 107.6(3)–110.8(3)°, and this boron is considered to act as a Lewis acid, engaged in a dative bond from nickel to boron. Whereas the S–Ni–Cl angles in $\text{Tm}^{\text{R}}\text{NiCl}$ (113.52(2)–114.00(3)°) deviate only slightly from the ideal tetrahedral value, the corresponding values in the nickelaborat-

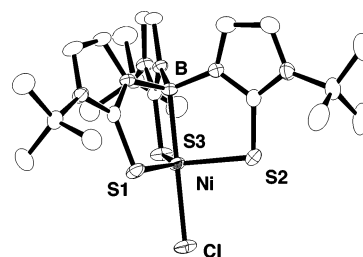
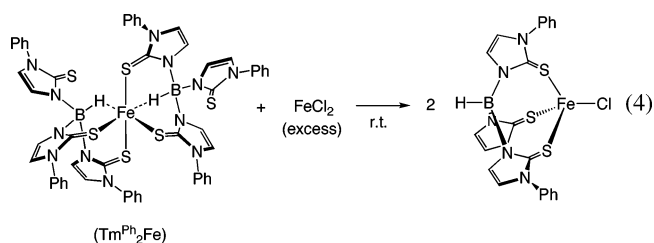


Figure 2. Molecular structure of $\{\text{B}(\text{timi}^{\text{tBu}})_3\}\text{NiCl}$. Selected bond distances (Å) and angles (deg): Ni–Cl 2.355(1), Ni–S(1) 2.259(2), Ni–S(2) 2.223(1), Ni–S(3) 2.267(1), Ni–B 2.108(4), B–Ni–S(1) 87.1(1), B–Ni–S(2) 87.7(1), B–Ni–S(3) 88.9(1), Cl–Ni–S(1) 93.76(4), Cl–Ni–S(2) 91.24(4), Cl–Ni–S(3) 91.38(4), S(1)–Ni–S(2) 137.77(5), S(1)–Ni–S(3) 103.61(5), S(2)–Ni–S(3) 118.17(5).

Mono{hydrotris(mercaptoimidazolyl)borato} Complexes

arane complex decrease to 91.24(4)–93.76(4)°. These values are in agreement with the trigonal bipyramidal arrangement at the nickel, but three equatorial sulfur atoms are not arranged in an ideal trigonal manner, with the S–Ni–S angles ranging 103.61(5)–137.77(5)°.

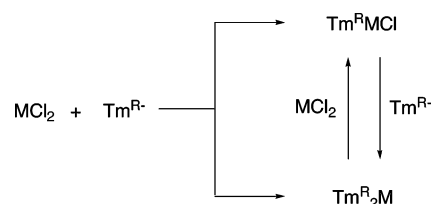
Formation of $\text{Tm}^{\text{R}}\text{MCl}$ from $\text{Tm}^{\text{R}}_2\text{M}$ and MCl_2 . In the synthesis of $(\text{Tm}^{\text{R}}\text{MCl})_n$ ($n = 1, 2$), the use of excess MCl_2 toward the Tm^{R} anion and the prolonged reaction time was found to be important. Therefore, we suggested that the sandwich complex, $\text{Tm}^{\text{R}}_2\text{M}$, would be converted to $(\text{Tm}^{\text{R}}\text{MCl})_n$ ($n = 1, 2$) in the presence of excess MCl_2 .



Treatment of the known sandwich complex, $\text{Tm}^{\text{Ph}}_2\text{Fe}$,¹⁰ with excess FeCl_2 at room temperature led to a gradual color change from dark green to green over the period of 12 h. After removal of the excess FeCl_2 , $\text{Tm}^{\text{Ph}}\text{FeCl}$ was obtained as a green powder in 80% yield. Taking this result into account, we propose that the initial reaction mixture of the Tm^{R} anion and excess MCl_2 includes both $\text{Tm}^{\text{R}}\text{MCl}$ and $\text{Tm}^{\text{R}}_2\text{M}$. The sandwich complex $\text{Tm}^{\text{R}}_2\text{M}$ gradually reacts with excess MCl_2 to form $\text{Tm}^{\text{R}}\text{MCl}$ (Scheme 1). This hypothesis is also in agreement with the dominant formation of $\text{Tm}^{\text{Me}}_2\text{-Ni}$ in the reaction of NaTm^{Me} with 5 equiv of NiCl_2 . The formed $\text{Tm}^{\text{Me}}_2\text{Ni}$ complex is sparingly soluble in common organic solvents, and this prevents it from reacting with excess NiCl_2 to form $[\text{Tm}^{\text{Me}}\text{Ni}(\mu\text{-Cl})]_2$.

The reaction of $\text{Tm}^{\text{R}}_2\text{M}$ with MCl_2 requires the facile dissociation of the C=S and B–H groups followed by transfer of the ligand between the metal centers. As mentioned above, the C=S distance is not affected by the variety of the metals or the halides on the metals, indicating that the coordinated C=S groups would be labile. The flexibility of an eight-membered metallacycle would also be important for the ligand transfer. Although the liberation of the M–N or M–H–B interaction in the transition metal Tp_2M complexes is known, the ligand transfer reaction from Tp_2M to the metal halides has not appeared to date. The six-membered metallacycle in the Tp_2M complexes is less flexible, and the dissociated pyrazolyl group remains in the coordination sphere, whereas the eight-membered rings in the Tm^{R} complexes are flexible enough to let the liberated thioimidazolyl group interact with the external metal ions. This hypothesis is supported by the fact that $\text{Tm}^{\text{iBu}}\text{CoBr}$ is in equilibrium with the dimeric $[\text{Tm}^{\text{iBu}}_2\text{Co}_2\text{Br}]^+$ species, which has been crystallographically identified as the PF_6 salt.^{9a} Such a dinuclear species with bridging between the Tm^{R} ligands is a possible intermediate during the reaction of $\text{Tm}^{\text{R}}_2\text{M}$ with

Scheme 1



MCl_2 . The ligand redistribution reaction has been recently demonstrated for the Tm^{Et} complexes.¹³

General Procedures. All reactions and the manipulations of the transition metal complexes were performed under a nitrogen atmosphere using standard Schlenk techniques. Solvents were dried, degassed, and distilled from sodium/benzophenone ketyl (hexane, ether, THF, toluene), from CaH_2 (CH_2Cl_2) or from Mg turnings (MeOH) under nitrogen, except for CHCl_3 (used as purchased).

The ^1H NMR spectra were acquired using a Varian INOVA-500 spectrometer. The spectra were referenced to the residual proton resonance of CDCl_3 . The infrared spectra were recorded using a Perkin-Elmer 2000 Fourier transform (FT) IR spectrometer or a JASCO A3 spectrometer. Elemental analyses for C, H, N, and S were performed using a LECO CHNS-932 elemental analyzer where the crystalline samples were sealed in silver capsules under a nitrogen atmosphere. Fast atom bombardment (FAB) mass spectra were obtained on a JEOL JMS-LCMATE mass spectrometer under a stream of high energy Xe gas, where 3-nitrobenzyl alcohol was used as the matrix. UV–vis spectra were measured using a JASCO V560 spectrometer. X-ray diffraction data were collected using a Rigaku AFC7R/Mercury charge-coupled device (CCD) system or a Rigaku AFC7R/ADSC Quantum 1 CCD system equipped with a rotating anode using graphite-monochromated Mo $\text{K}\alpha$ radiation. Transition metal halides and the other reagents were purchased and used without further purification. The following compounds were prepared according to the literature procedures: NaTm^{Me} ,^{4b} LiTm^{iBu} ,^{7d} and LiTm^{Ph} .^{7a} Repeated attempts to obtain satisfactory elemental analysis for $(\text{Tm}^{\text{Me}}\text{FeCl})_n$ ($n = 1$ or 2), $[\text{Tm}^{\text{Me}}\text{M}(\mu\text{-Cl})]_2$ ($\text{M} = \text{Mn}, \text{Co}, \text{Ni}$), $\text{Tm}^{\text{Ph}}\text{MCl}$ ($\text{M} = \text{Fe}, \text{Mn}, \text{Co}, \text{Ni}$), $\text{Tm}^{\text{iBu}}\text{MnCl}$, $\text{Tm}^{\text{Ar}}\text{MCl}$ ($\text{M} = \text{Co}, \text{Ni}$), $\text{Tm}^{\text{Ph}}\text{MI}$ ($\text{M} = \text{Co}, \text{Ni}$), $\{\text{B}(\text{timi}^{\text{iBu}})_3\}\text{NiCl}$, and $(\text{Htimi}^{\text{iBu}})_2\text{NiCl}_2$, even with the use of single crystals, were unsuccessful to fit within the standards, probably due to the contamination of a small amount of crystal solvent. The crystals used for the elemental analysis were ground down in a glovebox and left under reduced pressure prior to sealing in silver capsules.

Synthesis of LiTm^{Ar} ($\text{Ar} = 2,6\text{-iPr}_2\text{C}_6\text{H}_3$). A mixture of 2,6-diisopropylphenylthiocyanate (29.6 g, 135 mmol) and $\text{NH}_2\text{CH}_2\text{CH}(\text{OEt})_2$ (18.0 g, 135 mmol) in toluene (60 mL) was stirred at room temperature for 3 h. After the addition of concentrated HCl (6.3 mL), the reaction mixture was refluxed for 12 h to afford a brown solid. The solid was suspended in water (100 mL), and the solution was neutralized with 0.2 M NaOH. The solid was dissolved into CHCl_3 ,

(13) Bailey, P. J.; Dawson, A.; McCormack, C.; Moggach, S. A.; Oswald, I. D. H.; Parsons, S.; Rankin, D. W. H.; Turner, A. *Inorg. Chem.* **2005**, *44*, 8884–8898.

and the organic extracts were dried over Na_2SO_4 ; then the solvent was removed under reduced pressure to give a white crystalline solid. The vacuum-dried 2-mercapto-1-(2,6-diisopropylphenyl)imidazole (11.9 g, 34%) is sufficiently pure to be used in the following step. ^1H NMR (CDCl_3 , rt, δ): 1.11 (d, $J = 7.0$ Hz, 6H, ^iPr), 1.28 (d, $J = 7.0$ Hz, 6H, ^iPr), 2.58 (sep, $J = 7.0$ Hz, ^iPr), 6.64 (d, $J = 2.0$ Hz, 1H, CH), 6.85 (d, $J = 2.0$ Hz, 1H, CH), 7.27 (d, $J = 3.0$ Hz, 2H, $m\text{-Ph}$), 7.45 (t, $J = 3.0$ Hz, 1H, $p\text{-Ph}$).

To a toluene solution (90 mL) of 2-mercapto-1-(2,6-diisopropylphenyl)imidazole (10.25 g, 39.4 mmol) was added LiBH_4 (0.286 g, 13.2 mmol), and the mixture was refluxed under argon for 12 h. The resulting white solid was collected under air and then washed with ether and dried under a vacuum to give LiTm^{Ar} (7.19 g, 77%) as a white solid. ^1H NMR (CDCl_3 , rt, δ): 1.06 (d, $J = 6.5$ Hz, 18H, ^iPr), 1.16 (d, $J = 6.5$ Hz, 18H, ^iPr), 2.56 (sep, $J = 6.5$ Hz, 3H, ^iPr), 6.41 (d, $J = 2.0$ Hz, 1H, CH), 6.68 (d, $J = 2.0$ Hz, 1H, CH), 7.20 (d, $J = 2.5$ Hz, 2H, $m\text{-Ph}$), 7.39 (t, $J = 2.5$ Hz, $p\text{-Ph}$). IR (KBr, cm^{-1}): 2397 (B–H). Anal. Calcd for $\text{C}_{45}\text{H}_{58}\text{N}_6\text{S}_3\text{BLi}$: C, 67.82; H, 7.34; N, 10.55; S, 12.07. Found: C, 67.78; H, 7.40; N, 10.47; S, 11.96.

Synthesis of $(\text{Tm}^{\text{Me}}\text{FeCl})_n$ ($n = 1$ or 2). To a stirred suspension of NaTm^{Me} (0.300 g, 0.80 mmol) in CH_2Cl_2 (30 mL) was added anhydrous FeCl_2 (0.304 g, 2.40 mmol) at room temperature, and the mixture was then allowed to stir for 4 days. After the suspension was centrifuged to remove the NaCl and excess FeCl_2 , the solvent was removed under reduced pressure to afford a green solid. The green solid was repeatedly washed with hexane, giving rise to $(\text{Tm}^{\text{Me}}\text{FeCl})_n$ ($n = 1$ or 2) as a green powder (0.276 g, 78% based on $[\text{Tm}^{\text{Me}}]^-$, 26% based on FeCl_2). A green crystalline powder was obtained from a CH_2Cl_2 solution layered onto hexane. IR (KBr, cm^{-1}): 2438 (BH), 1558, 1460, 1377, 1203, 681. FABMS (CH_2Cl_2), m/z : 406.9 ($[\text{M}]^+ - \text{Cl}$). UV–vis (CH_2Cl_2 , rt; λ_{max} , nm) (ϵ , $\times 10^3 \text{ M}^{-1}\text{cm}^{-1}$): 614 (1.3), 406 (2.9), 306 (6.9), 264 (18.6).

Synthesis of $\text{Tm}^{\text{tBu}}\text{FeCl}$. A 100 mL flask was charged with FeCl_2 (0.077 g, 0.610 mmol) and LiTm^{tBu} (0.300 g, 0.610 mmol), and CH_2Cl_2 (50 mL) was added. The resultant dark yellow suspension was stirred for 4 days at ambient temperature. After the suspension was centrifuged to remove LiCl and a small amount of unreacted FeCl_2 and LiTm^{tBu} , the solvent was removed under reduced pressure to afford a light brown powder. This solid was repeatedly washed with hexane, giving rise to $\text{Tm}^{\text{tBu}}\text{FeCl}$ as a light brown powder (0.330 g, 94%). Light brown crystals were recrystallized from THF/hexane at room temperature. IR (KBr, cm^{-1}): 2408 (BH), 1567, 1417, 1361, 1195, 687. FABMS (CH_2Cl_2), m/z : 568.2 ($[\text{M}]^+$), 533.1 ($[\text{M}]^+ - \text{Cl}$). UV–vis (CH_2Cl_2 , rt; λ_{max} , nm) (ϵ , $\times 10^3 \text{ M}^{-1}\text{cm}^{-1}$): 421 (0.08), 357 (0.26), 276 (1.0). Anal. Calcd for $\text{C}_{21}\text{H}_{34}\text{N}_6\text{S}_3\text{BFCl}$: C, 44.34; H, 6.02; N, 14.77; S, 16.91. Found: C, 44.34; H, 6.34; N, 14.63; S, 17.15.

Synthesis of $\text{Tm}^{\text{Ph}}\text{FeCl}$. The reaction of anhydrous FeCl_2 (0.070 g, 0.551 mmol) with LiTm^{Ph} (0.300 g, 0.551 mmol) in CH_2Cl_2 (60 mL) for 4 days afforded $\text{Tm}^{\text{Ph}}\text{FeCl}$ as a dark green powder (0.299 g, 86%). Green crystals were obtained

from a CH_2Cl_2 solution layered onto hexane at room temperature. IR (KBr, cm^{-1}): 2431 (BH), 1596, 1498, 1366, 1189, 692. FABMS (CH_2Cl_2), m/z : 593.1 ($[\text{M}]^+ - \text{Cl}$). UV–vis (CH_2Cl_2 , rt; λ_{max} , nm) (ϵ , $\times 10^3 \text{ M}^{-1}\text{cm}^{-1}$): 646 (0.69), 446 (0.93), 361 (1.7).

Synthesis of $\text{Tm}^{\text{Ar}}\text{FeCl}$. This compound was prepared by the method for $\text{Tm}^{\text{tBu}}\text{FeCl}$. LiTm^{Ar} (0.300 g, 0.376 mmol) in CH_2Cl_2 (15 mL) was added to a CH_2Cl_2 suspension (20 mL) of anhydrous FeCl_2 (0.190 g, 1.50 mmol) at room temperature for 4 days. $\text{Tm}^{\text{Ar}}\text{FeCl}$ (0.330 g, 99% based on $[\text{Tm}^{\text{Ar}}]^-$, 25% based on FeCl_2) crystals were grown by layering hexane onto a THF solution at room temperature. IR (KBr, cm^{-1}): 2409 (BH), 1552, 1468, 1370, 1183, 690. FABMS (CH_2Cl_2), m/z : 880.5 ($[\text{M}]^+$), 845.5 ($[\text{M}]^+ - \text{Cl}$). UV–vis (CH_2Cl_2 , rt; λ_{max} , nm) (ϵ , $\times 10^3 \text{ M}^{-1}\text{cm}^{-1}$): 354 (0.32), 285 (1.5). Anal. Calcd for $\text{C}_{45}\text{H}_{58}\text{N}_6\text{S}_3\text{BFCl}$: C, 61.33; H, 6.63; N, 9.54; S, 10.92. Found: C, 61.20; H, 6.88; N, 9.11; S, 11.40.

Synthesis of $[\text{Tm}^{\text{Me}}\text{Mn}(\mu\text{-Cl})_2]$. To a stirred solution of NaTm^{Me} (1.00 g, 2.67 mmol) in MeOH (40 mL) was added $\text{MnCl}_2 \cdot 4\text{H}_2\text{O}$ (0.529 g, 2.67 mmol) at room temperature, and the mixture was allowed to stir for 1 h. After removal of the solvent, the product was extracted with CH_2Cl_2 (20 mL) and the solution was centrifuged. The solvent was removed under reduced pressure, and the residue was washed repeatedly with hexane, giving rise to $[\text{Tm}^{\text{Me}}\text{Mn}(\mu\text{-Cl})_2]$ as a white powder (0.633 g, 54%). Colorless crystals were obtained from a CH_2Cl_2 solution layered onto hexane at room temperature. IR (KBr, cm^{-1}): 2391 (BH), 1562, 1459, 1378, 1205, 681. FABMS (CH_2Cl_2), m/z : 406.5 ($1/2[\text{M}]^+ - \text{Cl}$). UV–vis (CH_2Cl_2 , rt; λ_{max} , nm) (ϵ , $\times 10^3 \text{ M}^{-1}\text{cm}^{-1}$): 261 (27.2).

Synthesis of $\text{Tm}^{\text{tBu}}\text{MnCl}$. A procedure similar to that for the case of $[\text{Tm}^{\text{Me}}\text{Mn}(\mu\text{-Cl})_2]$ was used. LiTm^{tBu} (0.227 g, 0.505 mmol) was added to $\text{MnCl}_2 \cdot 4\text{H}_2\text{O}$ (0.100 g, 0.505 mmol) in MeOH (20 mL), and the mixture was stirred at room temperature for 3 days. $\text{Tm}^{\text{tBu}}\text{MnCl}$ was isolated as a white powder (0.254 g, 89%). A colorless crystalline solid was obtained from a CH_2Cl_2 solution layered onto hexane at room temperature. IR (KBr, cm^{-1}): 2411 (BH), 1567, 1481, 1361, 1195, 688. FABMS (CH_2Cl_2), m/z : 532.1 ($[\text{M}]^+ - \text{Cl}$). UV–vis (CH_2Cl_2 , rt; λ_{max} , nm) (ϵ , $\times 10^3 \text{ M}^{-1}\text{cm}^{-1}$): 269 (22.0).

Synthesis of $\text{Tm}^{\text{Ph}}\text{MnCl}$. Synthesis was as in the case of $[\text{Tm}^{\text{Me}}\text{Mn}(\mu\text{-Cl})_2]$. To a MeOH suspension (10 mL) of LiTm^{Ph} (0.275 g, 0.505 mmol) was added $\text{MnCl}_2 \cdot 4\text{H}_2\text{O}$ (0.100 g, 0.505 mmol) in MeOH (10 mL) at room temperature for 4 days. $\text{Tm}^{\text{Ph}}\text{MnCl}$ was isolated as a white powder (0.110 g, 35%). Colorless crystals were obtained from a CH_2Cl_2 solution layered onto hexane at room temperature. IR (KBr, cm^{-1}): 2420 (BH), 1596, 1498, 1363, 1187, 692. FABMS (CH_2Cl_2), m/z : 592.2 ($[\text{M}]^+ - \text{Cl}$). UV–vis (CH_2Cl_2 , rt; λ_{max} , nm) (ϵ , $\times 10^3 \text{ M}^{-1}\text{cm}^{-1}$): 280 (16.7).

Synthesis of $\text{Tm}^{\text{Ar}}\text{MnCl}$. The same procedure as in the case of $[\text{Tm}^{\text{Me}}\text{Mn}(\mu\text{-Cl})_2]$ was used. To a MeOH solution (10 mL) of LiTm^{Ar} (0.500 g, 0.627 mmol) was added $\text{MnCl}_2 \cdot 4\text{H}_2\text{O}$ (0.124 g, 0.627 mmol) in MeOH (10 mL) at room temperature for 4 days. $\text{Tm}^{\text{Ar}}\text{MnCl}$ was isolated as a white powder (0.472 g, 86%). Colorless crystals were obtained

from a CH_2Cl_2 solution layered onto hexane at room temperature. IR (KBr, cm^{-1}): 2413 (BH), 1556, 1469, 1363, 1186, 690. FABMS (CH_2Cl_2), m/z : 844.5 ($[\text{M}]^+ - \text{Cl}$). UV-vis (CH_2Cl_2 , rt; λ_{max} , nm) (ϵ , $\times 10^3 \text{ M}^{-1}\text{cm}^{-1}$): 271 (28.6). Anal. Calcd for $\text{C}_{45}\text{H}_{58}\text{N}_6\text{S}_3\text{BMnCl}$: C, 61.39; H, 6.64; N, 9.55; S, 10.93. Found: C, 61.44; H, 6.51; N, 9.52; S, 10.78.

Synthesis of $\text{Tm}^{\text{Me}}\text{CoCl}$. This compound has been reported.^{9b} The reaction of anhydrous CoCl_2 (0.205 g, 1.60 mmol) with LiTm^{Me} (0.200 g, 0.534 mmol) in CH_2Cl_2 (40 mL) for 4 days afforded $\text{Tm}^{\text{Me}}\text{CoCl}$ as a light green powder (0.089 g, 37% based on $[\text{Tm}^{\text{Me}}]^-$, 12% based on CoCl_2). A green crystalline solid was obtained from a CH_2Cl_2 solution layered onto hexane. IR (KBr, cm^{-1}): 2410 (BH), 1562, 1462, 1381, 1203, 683. FABMS (CH_2Cl_2), m/z : 410.1 ($[\text{M}]^+ - \text{Cl}$). UV-vis (CH_2Cl_2 , rt; λ_{max} , nm) (ϵ , $\times 10^3 \text{ M}^{-1}\text{cm}^{-1}$): 697 (1.2), 371 (4.2).

Synthesis of $\text{Tm}^{\text{tBu}}\text{CoCl}$. This is a known compound.^{9a} Addition of LiTm^{tBu} (0.200 g, 0.407 mmol) to anhydrous CoCl_2 (0.052 g, 0.407 mmol) in CH_2Cl_2 (30 mL) was stirred at room temperature for 4 days. $\text{Tm}^{\text{tBu}}\text{CoCl}$ was isolated as a green powder (0.180 g, 77%). Green crystals were recrystallized from THF/hexane at room temperature. IR (KBr, cm^{-1}): 2410 (BH), 1565, 1481, 1361, 1193, 683. FABMS (CH_2Cl_2), m/z : 563.3 ($[\text{M}]^+ - \text{Cl}$). UV-vis (CH_2Cl_2 , rt; λ_{max} , nm) (ϵ , $\times 10^3 \text{ M}^{-1}\text{cm}^{-1}$): 738 (1.0), 701 (1.3), 665 (0.96), 369 (3.4). Anal. Calcd for $\text{C}_{21}\text{H}_{34}\text{N}_6\text{S}_3\text{BCoCl}$: C, 44.10; H, 5.99; N, 14.69; S, 16.82. Found: C, 43.72; H, 5.90; N, 14.63; S, 16.41.

Synthesis of $\text{Tm}^{\text{Ph}}\text{CoCl}$. $\text{Tm}^{\text{Ph}}\text{CoCl}$ was prepared by a procedure similar to that employed for $\text{Tm}^{\text{tBu}}\text{FeCl}$. To a CH_2Cl_2 suspension (10 mL) of LiTm^{Ph} (0.210 g, 0.385 mmol) was added CoCl_2 (0.150 g, 1.16 mmol) in CH_2Cl_2 (20 mL) at room temperature for 4 days. $\text{Tm}^{\text{Ph}}\text{CoCl}$ was isolated as a dark green powder (0.143 g, 59% based on $[\text{Tm}^{\text{Ph}}]^-$, 20% based on CoCl_2). Green crystals were obtained from a CH_2Cl_2 solution layered onto hexane at room temperature. IR (KBr, cm^{-1}): 2418 (BH), 1596, 1498, 1367, 1190, 692. FABMS (CH_2Cl_2), m/z : 596.2 ($[\text{M}]^+ - \text{Cl}$). UV-vis (CH_2Cl_2 , rt; λ_{max} , nm) (ϵ , $\times 10^3 \text{ M}^{-1}\text{cm}^{-1}$): 740 (0.63), 702 (0.85), 663 (0.64), 371 (2.2), 279 (7.9).

Synthesis of $\text{Tm}^{\text{Ar}}\text{CoCl}$. A similar procedure as that for $\text{Tm}^{\text{tBu}}\text{FeCl}$ was used. The reaction of anhydrous CoCl_2 (0.300 g, 2.31 mmol) with LiTm^{Ar} (0.614 g, 0.770 mmol) in CH_2Cl_2 (30 mL) for 4 days afforded $\text{Tm}^{\text{Ar}}\text{CoCl}$ as a light blue powder (0.375 g, 55% based on $[\text{Tm}^{\text{Ar}}]^-$, 18% based on CoCl_2). Blue crystals were obtained from a CH_2Cl_2 solution layered onto hexane at room temperature. IR (KBr, cm^{-1}): 2440 (BH), 1558, 1471, 1369, 1183, 690. FABMS (CH_2Cl_2), m/z : 848.5 ($[\text{M}]^+ - \text{Cl}$). UV-vis (CH_2Cl_2 , rt; λ_{max} , nm) (ϵ , $\times 10^3 \text{ M}^{-1}\text{cm}^{-1}$): 738 (0.10), 701 (0.14), 665 (0.09), 369 (0.35).

Synthesis of $[\text{Tm}^{\text{Me}}\text{Ni}(\mu\text{-Cl})_2]$. This compound was prepared using a procedure similar to that adopted for $[\text{Tm}^{\text{Me}}\text{Mn}(\mu\text{-Cl})_2]$. To a CH_2Cl_2 solution (20 mL) of NaTm^{Me} (0.300 g, 0.801 mmol) was added anhydrous NiCl_2 (0.572 g, 4.15 mmol) in CH_2Cl_2 (20 mL) at room temperature for 4 days. $[\text{Tm}^{\text{Me}}\text{Ni}(\mu\text{-Cl})_2]$ was isolated as a green powder (0.065 g, 18% based on $[\text{Tm}^{\text{Me}}]^-$, 3.5% based on NiCl_2). Green crystals

were obtained from a $\text{CH}_2\text{Cl}_2/\text{CH}_3\text{CN}$ solution layered onto hexane at room temperature. IR (KBr, cm^{-1}): 2387 (BH), 1560, 1458, 1373, 1207, 683. FABMS (CH_2Cl_2), m/z : 409.1 ($1/2[\text{M}]^+ - \text{Cl}$). UV-vis (CH_2Cl_2 , rt; λ_{max} , nm) (ϵ , $\times 10^3 \text{ M}^{-1}\text{cm}^{-1}$): 424 (4.2), 378 (4.3), 331 (4.6), 267 (12.5).

Synthesis of $[\text{Tm}^{\text{Me}}\text{Ni}(\mu\text{-Br})_2]$. A procedure similar to that for the case of $[\text{Tm}^{\text{Me}}\text{Mn}(\mu\text{-Cl})_2]$ was used. The reaction of anhydrous NiBr_2 (2.40 g, 10.7 mmol) with NaTm^{Me} (4.00 g, 10.7 mmol) in MeOH (100 mL) for 1 h afforded $[\text{Tm}^{\text{Me}}\text{Ni}(\mu\text{-Br})_2]$ as a dark brown powder (3.70 g, 71%). Brown crystals were obtained from a CH_2Cl_2 solution layered onto hexane at room temperature. IR (KBr, cm^{-1}): 2440 (BH), 1560, 1461, 1376, 1210. FABMS (CH_2Cl_2), m/z : 409.1 ($1/2[\text{M}]^+ - \text{Br}$). UV-vis (CH_2Cl_2 , rt; λ_{max} , nm) (ϵ , $\times 10^3 \text{ M}^{-1}\text{cm}^{-1}$): 731 (4.6), 426 (6.7), 363 (7.1), 330 (7.6). Anal. Calcd for $\text{C}_{24}\text{H}_{32}\text{N}_{12}\text{S}_6\text{B}_2\text{Ni}_2\text{Br}_2$: C, 29.42; H, 3.29; N, 17.15; S, 19.67. Found: C, 29.66; H, 2.97; N, 17.37; S, 19.89.

Synthesis of $\text{Tm}^{\text{Ph}}\text{NiCl}$. This compound was prepared using the same procedure described above for $\text{Tm}^{\text{tBu}}\text{FeCl}$. Addition of LiTm^{Ph} (0.300 g, 0.551 mmol) to anhydrous NiCl_2 (0.393 g, 1.65 mmol) in CH_2Cl_2 (50 mL) was stirred at room temperature for 4 days. $\text{Tm}^{\text{Ph}}\text{NiCl}$ was isolated as a green powder (0.193 g, 55% based on $[\text{Tm}^{\text{Ph}}]^-$, 19% based on NiCl_2). Green crystals were obtained from a CH_2Cl_2 solution layered onto hexane at room temperature. IR (KBr, cm^{-1}): 2431 (BH), 1596, 1498, 1364, 1189, 692. FABMS (CH_2Cl_2), m/z : 595.2 ($[\text{M}]^+ - \text{Cl}$). UV-vis (CH_2Cl_2 , rt; λ_{max} , nm) (ϵ , $\times 10^3 \text{ M}^{-1}\text{cm}^{-1}$): 730 (0.38), 640 (0.45), 392 (3.9).

Synthesis of $\text{Tm}^{\text{Ar}}\text{NiCl}$. Synthesis was as in the case of $\text{Tm}^{\text{tBu}}\text{FeCl}$. To a CH_2Cl_2 suspension (10 mL) of LiTm^{Ar} (4.00 g, 5.02 mmol) was added NiCl_2 (4.77 g, 20.1 mmol) in CH_2Cl_2 (20 mL) at room temperature for 4 days. $\text{Tm}^{\text{Ar}}\text{NiCl}$ was isolated as a yellowish green powder (3.52 g, 79% based on $[\text{Tm}^{\text{Ar}}]^-$, 20% based on NiCl_2). Yellowish green crystals were obtained from a CH_2Cl_2 solution layered onto hexane at room temperature. IR (KBr, cm^{-1}): 2439 (BH), 1550, 1470, 1371, 1190, 690. FABMS (CH_2Cl_2), m/z : 882.4 ($[\text{M}]^+$), 847.4 ($[\text{M}]^+ - \text{Cl}$). UV-vis (CH_2Cl_2 , rt; λ_{max} , nm) (ϵ , $\times 10^3 \text{ M}^{-1}\text{cm}^{-1}$): 450 (0.19), 384 (0.67), 284 (2.6).

Synthesis of $\text{Tm}^{\text{tBu}}\text{FeI}$. To a stirred solution of $\text{Tm}^{\text{tBu}}\text{FeCl}$ (0.150 g, 0.284 mmol) in THF (20 mL) was added NaI (0.047 g, 0.312 mmol) at room temperature, and the mixture was allowed to stir for 3 h. The solution immediately turned to a reddish brown suspension. After it was centrifuged to remove NaCl, the solvent was removed under reduced pressure to afford a brown solid. The brown solid was washed repeatedly with hexane and ether to afford $\text{Tm}^{\text{tBu}}\text{FeI}$ as a brown powder (0.175 g, 93%). Brown crystals were obtained from a CH_2Cl_2 solution layered onto hexane at room temperature. IR (KBr, cm^{-1}): 2424 (BH), 1565, 1481, 1361, 1195, 692. FABMS (CH_2Cl_2), m/z : 534.3 ($[\text{M}]^+ - \text{I}$). UV-vis (CH_2Cl_2 , rt; λ_{max} , nm) (ϵ , $\times 10^3 \text{ M}^{-1}\text{cm}^{-1}$): 361 (10.7), 286 (29.5). Anal. Calcd for $\text{C}_{21}\text{H}_{34}\text{N}_6\text{S}_3\text{BFeI}$: C, 38.20; H, 5.19; N, 12.73; S, 14.57. Found: C, 38.09; H, 5.32; N, 12.63; S, 14.08.

Synthesis of $\text{Tm}^{\text{Ph}}\text{FeI}$. This compound was prepared by the method for $\text{Tm}^{\text{tBu}}\text{FeI}$. To a THF solution (10 mL) of NaI (0.098 g, 0.655 mmol) was added $\text{Tm}^{\text{Ph}}\text{FeCl}$ (0.412 g,

0.655 mmol) in THF (20 mL) at room temperature for 3 h. $\text{Tm}^{\text{Ph}}\text{FeI}$ was isolated as a dark green powder (0.304 g, 64%). Green crystals were obtained from a CH_2Cl_2 solution layered onto hexane at room temperature. IR (KBr, cm^{-1}): 2431 (BH), 1556, 1496, 1359, 1189, 692. FABMS (CH_2Cl_2), m/z : 593.2 ($[\text{M}]^+ - \text{I}$). UV-vis (CH_2Cl_2 , rt; λ_{max} , nm) (ϵ , $\times 10^3 \text{ M}^{-1}\text{cm}^{-1}$): 646 (2.1), 446 (4.8), 290 (16.9). Anal. Calcd for $\text{C}_{27}\text{H}_{22}\text{N}_6\text{S}_3\text{BFeI}$: C, 45.02; H, 3.08; N, 11.67; S, 13.36. Found: C, 44.75; H, 3.09; N, 11.68; S, 13.03.

Synthesis of $\text{Tm}^{\text{Ar}}\text{FeI}$. The same procedure as in the case of $\text{Tm}^{\text{tBu}}\text{FeI}$ was used. To a THF suspension (10 mL) of NaI (0.034 g, 0.227 mmol) was added $\text{Tm}^{\text{Ar}}\text{FeCl}$ (0.200 g, 0.227 mmol) in THF (20 mL) at room temperature for 3 h. $\text{Tm}^{\text{Ar}}\text{FeI}$ was isolated as a dark yellow powder (0.122 g, 55%). Yellow crystals were recrystallized from THF/hexane at room temperature. IR (KBr, cm^{-1}): 2424 (BH), 1553, 1470, 1366, 1184, 689. FABMS (CH_2Cl_2), m/z : 845.4 ($[\text{M}]^+ - \text{I}$). UV-vis (CH_2Cl_2 , rt; λ_{max} , nm) (ϵ , $\times 10^3 \text{ M}^{-1}\text{cm}^{-1}$): 341 (4.1). Anal. Calcd for $\text{C}_{45}\text{H}_{58}\text{N}_6\text{S}_3\text{BFeI}$: C, 55.56; H, 6.01; N, 8.64; S, 9.89. Found: C, 55.33; H, 6.05; N, 8.39; S, 9.61.

Synthesis of $\text{Tm}^{\text{tBu}}\text{MnI}$. $\text{Tm}^{\text{tBu}}\text{MnI}$ was prepared by a procedure similar to that employed for $\text{Tm}^{\text{tBu}}\text{FeI}$. Addition of NaI (0.053 g, 0.353 mmol) to $\text{Tm}^{\text{tBu}}\text{MnCl}$ (0.200 g, 0.352 mmol) in THF (20 mL) was stirred at room temperature for 1 day. $\text{Tm}^{\text{tBu}}\text{MnI}$ was isolated as a white powder (0.220 g, 95%). Colorless crystals were obtained from a CH_2Cl_2 solution layered onto hexane at room temperature. IR (KBr, cm^{-1}): 2414 (BH), 1567, 1481, 1361, 1195, 686. FABMS (CH_2Cl_2), m/z : 532.3 ($[\text{M}]^+ - \text{I}$). UV-vis (CH_2Cl_2 , rt; λ_{max} , nm) (ϵ , $\times 10^3 \text{ M}^{-1}\text{cm}^{-1}$): 274 (19.4). Anal. Calcd for $\text{C}_{21}\text{H}_{34}\text{N}_6\text{S}_3\text{BMnI}$: C, 38.25; H, 5.20; N, 12.75; S, 14.59. Found: C, 38.12; H, 5.29; N, 12.46; S, 14.86.

Synthesis of $\text{Tm}^{\text{Ph}}\text{MnI}$. A similar procedure as that for $\text{Tm}^{\text{tBu}}\text{FeI}$ was used. The reaction of $\text{Tm}^{\text{Ph}}\text{MnCl}$ (0.218 g, 0.384 mmol) with NaI (0.058 g, 0.384 mmol) in THF (20 mL) for 1 day afforded $\text{Tm}^{\text{Ph}}\text{MnI}$ as a white powder (0.257 g, 93%). Colorless crystals were obtained from a CH_2Cl_2 solution layered onto hexane at room temperature. IR (KBr, cm^{-1}): 2422 (BH), 1594, 1498, 1367, 1189, 692. FABMS (CH_2Cl_2), m/z : 592.2 ($[\text{M}]^+ - \text{I}$). UV-vis (CH_2Cl_2 , rt; λ_{max} , nm) (ϵ , $\times 10^3 \text{ M}^{-1}\text{cm}^{-1}$): 278 (13.2). Anal. Calcd for $\text{C}_{27}\text{H}_{22}\text{N}_6\text{S}_3\text{BMnI}$: C, 45.08; H, 3.08; N, 11.68; S, 13.37. Found: C, 44.79; H, 3.27; N, 11.56; S, 12.90.

Synthesis of $\text{Tm}^{\text{Ar}}\text{MnI}$. This compound was prepared using a procedure similar to that adopted for $\text{Tm}^{\text{tBu}}\text{FeI}$. To a THF solution (10 mL) of NaI (0.125 g, 0.831 mmol) was added $\text{Tm}^{\text{Ar}}\text{MnCl}$ (0.472 g, 0.536 mmol) in THF (10 mL) at room temperature for 1 day. $\text{Tm}^{\text{Ar}}\text{MnI}$ was isolated as a white powder (0.395 g, 76%). Colorless crystals were recrystallized from THF/hexane at room temperature. IR (KBr, cm^{-1}): 2435 (BH), 1560, 1471, 1369, 1187, 690. FABMS (CH_2Cl_2), m/z : 844.5 ($[\text{M}]^+ - \text{I}$). UV-vis (CH_2Cl_2 , rt; λ_{max} , nm) (ϵ , $\times 10^3 \text{ M}^{-1}\text{cm}^{-1}$): 275 (28.5). Anal. Calcd for $\text{C}_{45}\text{H}_{58}\text{N}_6\text{S}_3\text{BMnI}$: C, 55.62; H, 6.02; N, 8.65; S, 9.90. Found: C, 55.73; H, 6.36; N, 8.54; S, 9.61.

Synthesis of $\text{Tm}^{\text{tBu}}\text{CoI}$. This compound was prepared using the same procedure described above for $\text{Tm}^{\text{tBu}}\text{FeI}$. Addition of NaI (0.052 g, 0.350 mmol) to $\text{Tm}^{\text{tBu}}\text{CoCl}$ (0.200

g, 0.350 mmol) in THF (30 mL) was stirred at room temperature for 3 h. $\text{Tm}^{\text{tBu}}\text{CoI}$ was isolated as a light yellow powder (0.216 g, 93%). IR (KBr, cm^{-1}): 2411 (BH), 1595, 1498, 1363, 1186, 692. FABMS (CH_2Cl_2), m/z : 536.3 ($[\text{M}]^+ - \text{I}$). UV-vis (CH_2Cl_2 , rt; λ_{max} , nm) (ϵ , $\times 10^3 \text{ M}^{-1}\text{cm}^{-1}$): 758 (0.98), 740 (0.91), 695 (0.78), 393 (2.5). Anal. Calcd for $\text{C}_{21}\text{H}_{34}\text{N}_6\text{S}_3\text{BCoI}$: C, 38.02; H, 5.17; N, 12.67; S, 14.50. Found: C, 37.85; H, 5.36; N, 12.31; S, 14.29.

Synthesis of $\text{Tm}^{\text{Ph}}\text{CoI}$. The same procedure as in the case of $\text{Tm}^{\text{tBu}}\text{FeI}$ was used. To a THF suspension (10 mL) of NaI (0.034 g, 0.226 mmol) was added $\text{Tm}^{\text{Ph}}\text{CoCl}$ (0.143 g, 0.226 mmol) in THF (20 mL) at room temperature for 3 h. $\text{Tm}^{\text{Ph}}\text{CoI}$ was isolated as a green powder (0.075 g, 46%). Green crystals were obtained from a CH_2Cl_2 solution layered onto hexane at room temperature. IR (KBr, cm^{-1}): 2436 (BH), 1595, 1498, 1366, 1190, 690. FABMS (CH_2Cl_2), m/z : 596.2 ($[\text{M}]^+ - \text{I}$). UV-vis (CH_2Cl_2 , rt; λ_{max} , nm) (ϵ , $\times 10^3 \text{ M}^{-1}\text{cm}^{-1}$): 761 (1.0), 730 (0.86), 694 (0.65), 393 nm (2.5).

Synthesis of $\text{Tm}^{\text{Ar}}\text{CoI}$. A similar procedure as that for $\text{Tm}^{\text{tBu}}\text{FeI}$ was used. The reaction of $\text{Tm}^{\text{Ar}}\text{CoCl}$ (0.164 g, 0.185 mmol) with NaI (0.028 g, 0.185 mmol) in CH_2Cl_2 (40 mL) for 3 h afforded $\text{Tm}^{\text{Ar}}\text{CoI}$ as a light yellowish green powder (0.136 g, 75%). Yellowish green crystals were obtained from a CH_2Cl_2 solution layered onto hexane at room temperature. IR (KBr, cm^{-1}): 2436 (BH), 1553, 1470, 1366, 1185, 690. FABMS (CH_2Cl_2), m/z : 848.5 ($[\text{M}]^+ - \text{I}$). UV-vis (CH_2Cl_2 , rt; λ_{max} , nm) (ϵ , $\times 10^3 \text{ M}^{-1}\text{cm}^{-1}$): 759 (0.11), 406 (0.92), 269 (17.2). Anal. Calcd for $\text{C}_{45}\text{H}_{58}\text{N}_6\text{S}_3\text{BCoI}$: C, 59.63; H, 7.55; N, 7.32; S, 8.38. Found: C, 59.43; H, 7.57; N, 7.06; S, 7.89.

Synthesis of $\text{Tm}^{\text{Ph}}\text{NiI}$. Synthesis was as in the case of $\text{Tm}^{\text{tBu}}\text{FeI}$. Addition of NaI (0.052 g, 0.348 mmol) to $\text{Tm}^{\text{Ph}}\text{NiCl}$ (0.200 g, 0.317 mmol) in THF (60 mL) was stirred at room temperature for 3 h. $\text{Tm}^{\text{Ph}}\text{NiI}$ was isolated as an orange powder (0.198 g, 86%). Orange crystals were obtained from a CH_2Cl_2 solution layered onto hexane at room temperature. IR (KBr, cm^{-1}): 2413 (BH), 1554, 1469, 1367, 1183, 690. FABMS (CH_2Cl_2), m/z : 595.2 ($[\text{M}]^+ - \text{I}$). UV-vis (CH_2Cl_2 , rt; λ_{max} , nm) (ϵ , $\times 10^3 \text{ M}^{-1}\text{cm}^{-1}$): 784 (0.35), 699 (0.45), 411 (4.8).

Synthesis of $\text{Tm}^{\text{Ar}}\text{NiI}$. This compound was prepared by the method for $\text{Tm}^{\text{tBu}}\text{FeI}$. To a THF solution (10 mL) of NaI (0.034 g, 0.226 mmol) was added $\text{Tm}^{\text{Ar}}\text{NiCl}$ (0.200 g, 0.226 mmol) in THF (10 mL) at room temperature for 3 h. $\text{Tm}^{\text{Ar}}\text{NiI}$ was isolated as an orange brown powder (0.153 g, 69%). Orange crystals were recrystallized from THF/hexane at room temperature. IR (KBr, cm^{-1}): 2435 (BH), 1551, 1471, 1369, 1187, 689. FABMS (CH_2Cl_2), m/z : 848.5 ($[\text{M}]^+ - \text{I}$). UV-vis (CH_2Cl_2 , rt; λ_{max} , nm) (ϵ , $\times 10^3 \text{ M}^{-1}\text{cm}^{-1}$): 402 (4.8), 273 (32.2). Anal. Calcd for $\text{C}_{45}\text{H}_{58}\text{N}_6\text{S}_3\text{BNiI}$: C, 55.40; H, 5.99; N, 8.61; S, 9.86. Found: C, 55.47; H, 6.01; N, 8.37; S, 9.47.

Formation of $\{\text{B}(\text{tim}^{\text{tBu}})_3\}\text{NiCl}$ from NiCl_2 and $\text{Li-Tm}^{\text{tBu}}$. To a stirred solution of LiTm^{tBu} (0.200 g, 0.412 mmol) in CH_2Cl_2 (25 mL) was added anhydrous NiCl_2 (0.053 g, 0.412 mmol) at room temperature, and the mixture was allowed to stir for 2 days. The solution immediately turned

Table 4. Crystallographic Data for the Complexes Refined by TEXSAN or Crystals

	[Tm ^{Mn} Mn(μ-Cl)] ₂	Tm ^{Pb} MnCl·3CH ₂ Cl ₂	Tm ^{Ar} MnCl·4.5CH ₂ Cl ₂	Tm ^{Pb} FeCl·3CH ₂ Cl ₂	Tm ^{Ar} FeCl·0.5(C ₄ H ₈ O)
formula	C ₁₂ H ₁₆ N ₆ S ₃ ClMn	C ₂₇ H ₂₂ N ₆ S ₃ BClMn·3CH ₂ Cl ₂	C ₄₅ H ₅₈ N ₆ S ₃ BClMn·4.5CH ₂ Cl ₂	C ₂₇ H ₂₂ N ₆ S ₃ BClFe·3CH ₂ Cl ₂	C ₄₅ H ₅₈ N ₆ S ₃ BClFe·0.5C ₄ H ₈ O
fw	441.68	882.69	1260.56	883.60	917.34
crystal system	monoclinic	trigonal	trigonal	trigonal	triclinic
space group	<i>P2₁/c</i>	<i>R3</i>	<i>P3c1</i>	<i>R3</i>	<i>P1</i>
<i>a</i> (Å)	10.087(2)	15.083(8)	19.501(4)	15.0294(4)	9.877(1)
<i>b</i> (Å)	10.001(2)				13.615(2)
<i>c</i> (Å)	19.205(5)	29.75(2)	19.687(4)	29.929(1)	18.340(2)
α (deg)					95.185(3)
β (deg)	103.169(3)				95.765(1)
δ (deg)					97.082(2)
<i>V</i> (Å ³)	1886.5(7)	5861(5)	6483.5(2)	5854.7(3)	2421.7(5)
<i>Z</i>	4	6	4	6	2
<i>D</i> _{calcd} (g/cm ³)	1.555	1.500	1.291	1.504	1.258
μ (cm ⁻¹)	11.80	10.07	7.48	10.56	5.35
<i>F</i> ₀₀₀	900	2682	2608	2760	972
max 2θ (deg)	55.0	62.3	55.0	55.1	55.1
no. of reflections					
collected	14854	17571	51205	21228	10839
indep	4301	3836	4966	2999	10391
no. of observations	4288 [<i>I</i> > 0σ(<i>I</i>)]	2418 [<i>I</i> > σ(<i>I</i>)]	1502 [<i>I</i> > σ(<i>I</i>)]	2955 [<i>I</i> > 0σ(<i>I</i>)]	10391 [<i>I</i> > 0σ(<i>I</i>)]
no. of variables	217	149	205	145	534
GOF indicator ^a	1.00	2.09	1.31	2.71	1.53
<i>R</i> ^b	0.038	0.057	0.067	0.089	0.053
<i>Rw</i> ^c	0.044	0.083	0.096	0.116	0.059

	Tm ^{Tb} CoCl·1.5C ₄ H ₈ O	Tm ^{Pb} CoCl·3CH ₂ Cl ₂	Tm ^{Ar} CoCl·4.5CH ₂ Cl ₂	[Tm ^{Mn} Ni(μ-Cl)] ₂	[Tm ^{Mn} Ni(μ-Br)] ₂
formula	C ₂₁ H ₃₄ N ₆ S ₃ BClCo·1.5C ₄ H ₈ O	C ₂₇ H ₂₂ N ₆ S ₃ BClCo·3CH ₂ Cl ₂	C ₄₅ H ₅₈ N ₆ S ₃ BClCo·4.5CH ₂ Cl ₂	C ₁₂ H ₁₆ N ₆ S ₃ BClNi	C ₁₂ H ₁₆ N ₆ S ₃ BBrNi
fw	680.08	886.69	1264.55	445.44	489.89
crystal system	trigonal	trigonal	trigonal	monoclinic	monoclinic
space group	<i>R3c</i>	<i>R3</i>	<i>P3c1</i>	<i>P2₁/n</i>	<i>P2₁/n</i>
<i>a</i> (Å)	13.469(3)	15.026(1)	19.5212(4)	9.676(4)	9.7934(7)
<i>b</i> (Å)				13.022(5)	13.1652(4)
<i>c</i> (Å)	64.02(1)	29.712(3)	19.4927(4)	14.899(6)	14.8919(2)
α (deg)					
β (deg)				102.916(5)	102.9534(5)
γ (deg)					
<i>V</i> (Å ³)	10058(4)	5809.6(9)	6433.0(2)	1829(1)	1871.2(1)
<i>Z</i>	12	6	4	4	4
<i>D</i> _{calcd} (g/cm ³)	1.347	1.521	1.306	1.617	1.739
μ (cm ⁻¹)	8.108	11.19	8.15	15.56	35.21
<i>F</i> ₀₀₀	4308	2694	2616	912	984
max 2θ (deg)	55.0	55.0	55.0	55.0	55.1
no. of reflections					
collected	25587	15187	75986	14089	4026
indep	2576	2949	4944	4137	3498
no. of observations	2570 [<i>I</i> > 0σ(<i>I</i>)]	2896 [<i>I</i> > 0σ(<i>I</i>)]	4717 [<i>I</i> > 0σ(<i>I</i>)]	3365 [<i>I</i> > 3σ(<i>I</i>)]	3498 [<i>I</i> > 3σ(<i>I</i>)]
no. of variables	120	145	205	217	217
GOF indicator ^a	0.861	2.05	1.88	1.38	1.11
<i>R</i> ^b	0.062	0.089	0.086	0.035	0.030
<i>Rw</i> ^c	0.097	0.100	0.091	0.047	0.039

	Tm ^{Pb} NiCl·3CH ₂ Cl ₂	Tm ^{Ar} NiCl·4.5CH ₂ Cl ₂	Tm ^{Pb} MnI·3CH ₂ Cl ₂	Tm ^{Ar} FeI·0.5C ₄ H ₈ O	Tm ^{Pb} CoI·3CH ₂ Cl ₂
formula	C ₂₇ H ₂₂ N ₆ S ₃ BClNi·3CH ₂ Cl ₂	C ₄₅ H ₅₈ N ₆ S ₃ BClNi·4.5CH ₂ Cl ₂	C ₂₇ H ₂₂ N ₆ S ₃ BMnI·3CH ₂ Cl ₂	C ₄₅ H ₅₈ N ₆ S ₃ BFeI·0.5C ₄ H ₈ O	C ₂₇ H ₂₂ N ₆ S ₃ BCoI·3CH ₂ Cl ₂
fw	886.45	1264.32	968.09	1008.79	978.14
crystal system	trigonal	trigonal	trigonal	triclinic	trigonal
space group	<i>R3</i>	<i>P3c1</i>	<i>R3</i>	<i>P1</i>	<i>R3</i>
<i>a</i> (Å)	14.973(4)	19.5220(5)	15.052(2)	10.167(5)	15.010(1)
<i>b</i> (Å)				13.547(7)	
<i>c</i> (Å)	29.775(8)	19.6676(3)	30.392(4)	18.242(9)	30.252(4)
α (deg)				94.51(1)	
β (deg)				95.393(8)	
γ (deg)				97.788(8)	
<i>V</i> (Å ³)	5780.(3)	6391.3(2)	5962(1)	2467(2)	5902(1)
<i>Z</i>	6	4	6	2	6
<i>D</i> _{calcd} (g/cm ³)	1.528	1.294	1.617	1.358	1.651
μ (cm ⁻¹)	11.82	8.42	17.00	10.97	18.18
<i>F</i> ₀₀₀	2700	2620	2862	1044	2910
max 2θ (deg)	55.0	54.9	54.9	55.0	55.0
no. of reflections					
collected	15348	9467	16242	19787	15054
indep	2935	4956	3047	10787	3001
no. of observations	2932 [<i>I</i> > 0σ(<i>I</i>)]	3898 [<i>I</i> > 3σ(<i>I</i>)]	1611 [<i>I</i> > 3σ(<i>I</i>)]	10679 [<i>I</i> > 0σ(<i>I</i>)]	2997 [<i>I</i> > 0σ(<i>I</i>)]
no. of variables	210	206	161	520	145
GOF indicator ^a	1.34	4.31	1.14	1.51	1.17
<i>R</i> ^b	0.057	0.062	0.052	0.078	0.067
<i>Rw</i> ^c	0.085	0.086	0.074	0.079	0.067

Table 4. (Continued)

	Tm ^{Ar} CoI·4.5CH ₂ Cl ₂	Tm ^{Ar} NiI·0.5C ₄ H ₈ O	(Htimi ^{tBu}) ₂ NiCl ₂	{B(timi ^{tBu}) ₃ }NiCl·2CH ₂ Cl ₂
formula	C ₄₅ H ₅₈ N ₆ S ₃ BClCo·4.5CH ₂ Cl ₂	C ₄₅ H ₅₈ N ₆ S ₃ INi·0.5C ₄ H ₈ O	C ₁₄ H ₂₂ N ₄ S ₂ Cl ₂ Ni	C ₂₁ H ₃₃ N ₆ S ₃ BCINi·2CH ₂ Cl ₂
fw	1356.00	1011.64	442.10	741.55
crystal system	trigonal	triclinic	monoclinic	monoclinic
space group	<i>P</i> 3 <i>c</i> 1	<i>P</i> 1	<i>C</i> 2/ <i>c</i>	<i>P</i> 2 ₁ / <i>n</i>
<i>a</i> (Å)	19.5001(5)	10.183(7)	16.76(1)	13.935(6)
<i>b</i> (Å)		13.571(7)	8.575(5)	15.718(6)
<i>c</i> (Å)	20.0779(8)	18.114(9)	16.70(1)	15.801(7)
α (deg)		94.90(1)		
β (deg)		95.120(8)	125.169(6)	107.145(5)
γ (deg)		98.155(9)		
<i>V</i> (Å ³)	6611.8(4)	2456.0(1)	1961(2)	3307(2)
<i>Z</i>	4	2	4	4
<i>D</i> _{calcd} (g/cm ³)	1.362	1.368	1.497	1.489
μ (cm ⁻¹)	12.20	11.90	14.77	12.05
<i>F</i> ₀₀₀	2760	1048	920	1536
max 2θ (deg)	55.0	55.0	55.0	55.0
no. of reflections				
collected	49946	20092	7734	24948
indep	5019	10794	2223	7483
no. of observations	5014 [<i>I</i> > 0σ(<i>I</i>)]	10588 [<i>I</i> > 0σ(<i>I</i>)]	2198 [<i>I</i> > 0σ(<i>I</i>)]	5256 [<i>I</i> > 0σ(<i>I</i>)]
no. of variables	205	533	105	352
GOF indicator ^a	1.80	1.13	0.95	1.83
<i>R</i> ^b	0.081	0.044	0.032	0.050
<i>Rw</i> ^c	0.098	0.048	0.043	0.075

^a GOF = [Σw(|*F*_o| - |*F*_c|)²/(*N*_o - *N*_p)]^{1/2}, where *N*_o and *N*_p denote the number of data and parameters. ^b *R* = Σ||*F*_o| - |*F*_c||/Σ|*F*_o| (observed reflections). ^c *Rw* = [Σw(|*F*_o| - |*F*_c|)²]/Σw(*F*_o)²]^{1/2} (observed reflections).

to a green suspension. After it was centrifuged to remove LiCl (and unreacted NiCl₂), the solvent was removed under reduced pressure to afford a dark green solid, which was washed repeatedly with hexane to yield {B(timi^{tBu})₃}NiCl as a green powder (0.162 g, 69%). Green crystals were obtained from a CH₂Cl₂ solution layered onto hexane at room temperature. IR (KBr, cm⁻¹): 1560, 1452, 1371, 1192, 683. FABMS (CH₂Cl₂), *m/z*: 534.2 ([M]⁺ - Cl). UV-vis (CH₂-Cl₂, rt; λ_{max}, nm) (ε, × 10³ M⁻¹cm⁻¹): 612 (0.40), 459 (1.9), 342 (4.0). In this reaction, a small amount of (Htimi^{tBu})₂-NiCl₂ was also obtained as green crystals. This was identified by comparison of the spectral data with the authentic sample prepared from the reaction of NiCl₂ and Htimi^{tBu}.

Reaction of NiCl₂ with *tert*-Butyl Thioimidazole (Htimi^{tBu}). A 100 mL flask was charged with NiCl₂ (0.020 g, 0.159 mmol) and Htimi^{tBu} (0.050 g, 0.319 mmol), and CH₂Cl₂ (25 mL) was added. The resultant green suspension was stirred for 1 day at ambient temperature. After the suspension was centrifuged to remove a small amount of unreacted NiCl₂, the solvent was removed under reduced pressure to afford a light green powder. This solid was repeatedly washed with hexane, giving rise to (Htimi^{tBu})₂-NiCl₂ as a light green powder (0.053 g, 75%). Green crystals were obtained from a CH₂Cl₂ solution layered onto hexane at room temperature. IR (KBr, cm⁻¹): 3347 (NH), 1571, 1471, 1453, 1372, 1322, 1216, 684. FABMS (CH₂Cl₂), *m/z*: 405.1 ([M]⁺ - Cl). UV-vis (CH₂Cl₂, rt; λ_{max}, nm) (ε, × 10³ M⁻¹cm⁻¹): 432 (1.0), 342 (3.6), 319 (2.2), 267 nm (20.6).

Reaction of Tm^{Pb}₂Fe with FeCl₂. To a CH₂Cl₂ solution (50 mL) of Tm^{Pb}₂Fe (0.594 g, 0.525 mmol) was added anhydrous FeCl₂ (1.33 g, 10.5 mmol), and the suspension was stirred for 12 h. After centrifugation to remove excess FeCl₂, the solvent was removed under reduced pressure. The green residue was washed repeatedly with hexane and ether to give a dark green powder of Tm^{Pb}FeCl (0.525 g, 80%), which was identified by means of an infrared spectrum and

Table 5. Crystallographic Data for the Complexes Refined by SHELX-97

	Tm ^{tBu} FeCl·1.5C ₄ H ₈ O	Tm ^{tBu} FeI	Tm ^{Pb} NiI·3CH ₂ Cl ₂
formula	C ₂₁ H ₃₄ N ₆ S ₃ BClFe·1.5C ₄ H ₈ O	C ₂₁ H ₃₄ N ₆ S ₃ BFeI	C ₂₇ H ₂₂ N ₆ S ₃ INi·3CH ₂ Cl ₂
fw	675.98	660.28	977.90
crystal system	trigonal	trigonal	trigonal
space group	<i>R</i> 3 <i>c</i>	<i>R</i> 3 <i>c</i>	<i>R</i> 3
<i>a</i> (Å)	13.4412(5)	13.486(3)	14.897(7)
<i>c</i> (Å)	64.368(3)	66.72(1)	30.34(1)
<i>V</i> (Å ³)	10071.1(7)	10519(5)	5842(5)
<i>Z</i>	12	12	6
<i>D</i> _{calcd} (g/cm ³)	1.337	1.251	1.668
μ (cm ⁻¹)	7.47	15.06	18.94
<i>F</i> ₀₀₀	4284	4008	2916
max 2θ (deg)	55.0	55.0	55.0
no. of reflections			
collected	25445	26518	14999
indep	2576	2699	2992
no. of observations	2576	2699	2992
no. of variables	119	101	149
GOF indicator ^a	2.11	2.38	1.38
<i>R</i> ^b	0.066	0.085	0.078
<i>wR</i> ^c	0.242	0.293	0.203 ^c

^a GOF = [Σw(|*F*_o|² - |*F*_c|²)/(*N*_o - *N*_p)]^{1/2}, where *N*_o and *N*_p denote the number of data and parameters. ^b *R* = Σ||*F*_o| - |*F*_c||/Σ|*F*_o| (*I* > 0σ(*I*)). ^c *wR* = [Σw(*F*_o)² - *F*_c)²]/Σw(*F*_o)²]^{1/2} (all data).

X-ray fluorescence microanalysis. It was also identified by a crystallographic study using dark green crystals obtained from CH₂Cl₂ and hexane.

X-ray Crystal Structure Determination. Crystal data and refinement parameters for the structurally characterized complexes are summarized in Table 4. Single crystals were coated with oil (Immersion Oil, type B: Code 1248, Cargille Laboratories, Inc.) and mounted on loops. Diffraction data were collected at -80 °C under a cold nitrogen stream on a Rigaku AFC7R/Mercury CCD system or a Rigaku AFC7R/ADSC Quantum 1 CCD system by using graphite-monochromated Mo Kα radiation (λ = 0.710 690 Å). Four preliminary data frames were measured at ω = 0, 30, 60,

and 90°, each with a 0.5° increment of ω , to assess the crystal quality and preliminary unit cell parameters. The intensity images were also measured at 0.5° intervals of ω . The frame data were integrated using an MSC d*TREK program package (Quantum 1 CCD) or a Rigaku CrystalClear program package (Mercury CCD), and the data sets were corrected for absorption using a REQAB program. The calculations were performed with a TEXSAN program package for [Tm^{Mn}Mn(μ -Cl)]₂, Tm^{Ph}MnCl·3CH₂Cl₂, Tm^{Ar}-MnCl·4.5CH₂Cl₂, Tm^{Ph}FeCl·3CH₂Cl₂, Tm^{Ar}FeCl·0.5C₄H₈O, Tm^{Ph}CoCl·3CH₂Cl₂, Tm^{Ar}CoCl·4.5CH₂Cl₂, [Tm^{Mn}Ni(μ -Cl)]₂, [Tm^{Mn}Ni(μ -Br)]₂, Tm^{Ar}NiCl·4.5CH₂Cl₂, Tm^{Ph}MnI·3CH₂Cl₂, Tm^{Ar}FeI·0.5C₄H₈O, Tm^{Ph}CoI·3CH₂Cl₂, Tm^{Ar}CoI·4.5CH₂Cl₂, Tm^{Ar}NiI·0.5C₄H₈O, (Htimi^{tBu})₂NiCl₂, and {B(timi^{tBu})₃}NiCl·2CH₂Cl₂. The structures were solved by a direct method (SIR92 or SHELX-97) or Patterson methods (DIRDIF94 PATTY) and were refined by full-matrix least-squares (TEXSAN) on $|F|$. Tm^{tBu}FeCl·1.5C₄H₈O, Tm^{tBu}CoCl·1.5C₄H₈O, Tm^{Ph}NiCl·3CH₂Cl₂, Tm^{tBu}FeI, and Tm^{Ph}NiI·3CH₂Cl₂ were studied using a CrystalStructure crystallographic software package and were solved by direct methods using SHELXS-97. The structures of Tm^{tBu}CoCl·1.5C₄H₈O and Tm^{Ph}NiCl·3CH₂Cl₂ were refined by full-matrix least-squares (Crystals) on $|F|$. Tm^{tBu}FeCl·1.5C₄H₈O, Tm^{tBu}FeI, and Tm^{Ph}NiI·3CH₂Cl₂ were refined on $|F^2|$ by the full-matrix least-squares method using SHELXS-97. Anisotropic refinement was applied to all non-hydrogen atoms except for the disordered crystal solvents, and all hydrogen atoms except for B-H were put at the calculated positions. The crystal solvent CH₂Cl₂ was disordered in Tm^{Ph}NiCl·3CH₂Cl₂ (one of the chloride atoms of CH₂Cl₂, over two positions with 8:2 occupancy factors), Tm^{Ph}MnI·3CH₂Cl₂ (over two positions of chloride with 6:4 occupancy factors), and Tm^{Ph}NiI·3CH₂Cl₂ (one of the chloride atoms of CH₂Cl₂, over three

positions with 5:3:2 occupancy factors). As for Tm^{Ph}NiCl·3CH₂Cl₂ and Tm^{Ph}NiI·3CH₂Cl₂, anisotropic refinement could not assign hydrogen atoms on CH₂Cl₂. A residual density observed in the Tm^{Ph} complexes of Mn, Fe, and Co was most likely attributed to the disordered CH₂Cl₂ over six positions. It was not easy to determine and was not assigned any atoms. Tm^{Ar}MnCl·4.5CH₂Cl₂, Tm^{Ar}CoCl·4.5CH₂Cl₂, Tm^{Ar}NiCl·4.5CH₂Cl₂, and Tm^{Ar}CoI·4.5CH₂Cl₂ contained two kinds of CH₂Cl₂ (1.0 and 0.5 occupancy factors) as a crystal solvent, and no hydrogen atoms were assigned on 0.5CH₂Cl₂. Tm^{tBu}FeI included residual density, but it was hard to assign any atoms. The crystal solvent THF in Tm^{tBu}FeCl·1.5C₄H₈O, Tm^{Ar}FeCl·0.5(C₄H₈O), Tm^{tBu}CoCl·1.5C₄H₈O, Tm^{Ar}FeI·0.5(C₄H₈O), and Tm^{Ar}NiI·0.5(C₄H₈O) was disordered over two positions with 1:1 occupancy factors. The THF solvents in Tm^{tBu}CoCl·1.5C₄H₈O and Tm^{Ar}FeI·0.5(C₄H₈O) were refined as a rigid group. The iodide ligand in Tm^{Ar}NiI·0.5(C₄H₈O) was disordered over two close positions with 9:1 occupancy factors. Additional data are available as Supporting Information.

Acknowledgment. This research is supported by a Grant-in-Aid for Scientific Research (No. 14078211 and 17036020) from the Ministry of Education, Culture, Sports, Science, and Technology, Japan.

Supporting Information Available: X-ray crystallographic information files (CIF) for the structures of [Tm^{Mn}M(μ -Cl)]₂ (M = Mn, Ni), [Tm^{Mn}Ni(μ -Br)]₂, Tm^{tBu}MCl (M = Fe, Co), Tm^{Ph}MCl (M = Mn, Fe, Co, Ni), Tm^{Ar}MCl (M = Mn, Fe, Co, Ni), Tm^{tBu}-FeI, Tm^{Ph}MI (M = Mn, Co, Ni), Tm^{Ar}MI (M = Fe, Co, Ni), {B(timi^{tBu})₃}NiCl, and (Htimi^{tBu})₂NiCl₂. This material is available free of charge via the Internet at <http://pubs.acs.org>.

IC0610132